PHYSICAL REVIEW
LETTERS

VOLUME 2 JUNE 1, 1959 NUMBER 11

DYNAMIC NUCLEAR POLARIZATION

M. Abraham,* M. A. H. McCausland, and F. N. H. Robinson†
The Clarendon Laboratory, Oxford, England
(Received April 13, 1959; revised manuscript received May 8, 1959)

Saturation of the microwave electron paramagnetic resonance of impurities in various materials produces enhanced and reversed nuclear polarization throughout the material, an effect discovered by Erb, Motchane, and Übersfeld[1] and Abragam and Proctor.[2]

Figure 1 shows the levels in a magnetic field of a single electron spin loosely coupled to a nucleus of spin $\frac{1}{2}$. Full arrows denote the allowed transitions, presumably also the fastest relaxation processes. Saturation of the partially forbidden line A at a frequency $\nu_e - \nu_n$ leads to the population distribution shown in column A on the right of the figure. The resulting ratio of the populations of nuclear substates with m_I positive to those with it negative is

$$x_1 \approx (2+\Delta)/(2-\Delta) \approx 1+\Delta,$$

compared with the equilibrium ratio

$$x_0 \approx 1+\delta,$$

where Δ and δ are the electronic and nuclear Boltzmann factors. Saturation of B yields

$$x_2 \approx 1-\Delta.$$

Thus A leads to a positive enhancement Δ/δ and B to a reversal $-\Delta/\delta$.

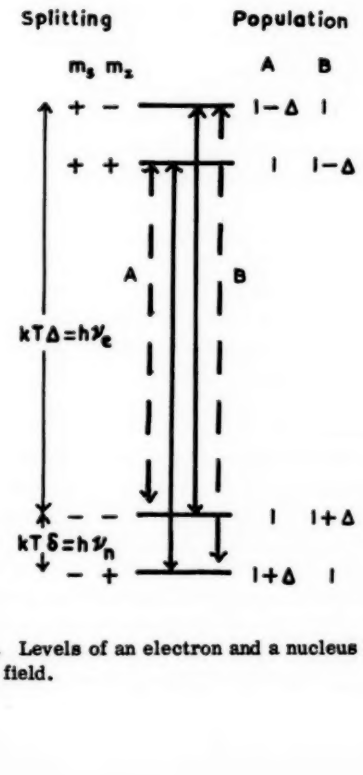

FIG. 1. Levels of an electron and a nucleus in a magnetic field.

In the materials investigated, the lines A and B are not resolved since their separation $2\nu_n$ is considerably less than the width $\Delta\nu_e$ of the electron line. If this is inhomogeneously broadened, a plot (Fig. 2) of the electron absorption line is equivalent to a plot of the number N of paramagnetic centers whose allowed frequency is ν in a particular field. An applied signal ν_0 saturates the allowed transition of N_0 centers, the transition A of N_1 centers whose allowed frequency is $\nu_0 + \nu_n$, and the transition B of N_2 centers. In the case illustrated, the net effect is a reversal depending on the difference between N_2 and N_1. The points of maximum enhancement and reversal coincide with the points of maximum slope of the

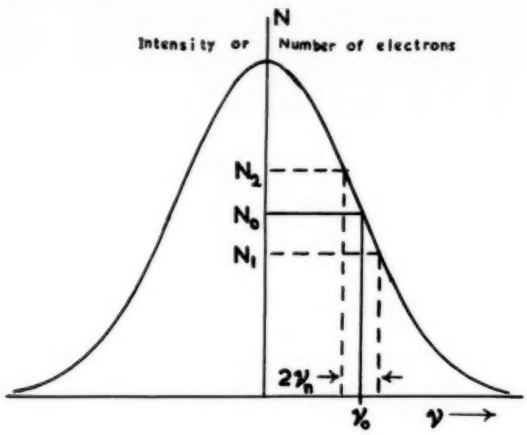

FIG. 2. Effect of electron line width.

electron absorption line. Enhancement at a fixed field occurs at electron frequencies below the line center (field above at fixed frequency), and reversal vice versa. For $\nu_n << \Delta\nu_e$, the maximum effect is proportional to $\nu_n/\Delta\nu_e$. Since the possible enhancement is $\Delta/\delta = \nu_e/\nu_n$, the over-all effect depends only on $\nu_e/\Delta\nu_e$ and not at all on the nuclear gyromagnetic ratio g_n.

In Fig. 3 we show the intensity at 1.6°K of the Li^7 nuclear resonance absorption signal in a single crystal of LiF containing F centers produced by x-rays. The microwave frequency is constant at 9.41 kMc/sec and the static magnetic field and nuclear resonance frequency are varied. Each point represents the ratio of the signal with the microwave power on to the signal in its absence. The signal-to-noise ratio of the unenhanced signal was greater than 5:1.

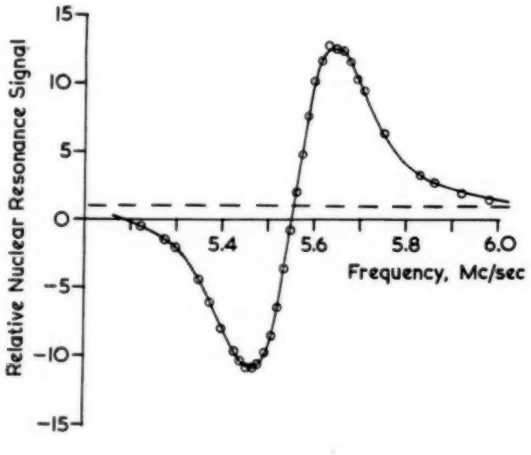

FIG. 3. Enhancement of Li nuclear resonance signal at 1.6°K as a function of the nuclear resonance frequency (or magnetic field) at a fixed microwave frequency 9.41 kMc/sec.

The results fit the theory outlined above, and the separation 0.18 Mc/sec or 108 gauss between the two maxima agrees well with the paramagnetic resonance result, 111 gauss, of Lord.[3] Exactly similar results obtain for the F^{19} resonance, confirming the independence of the effect on g_n. Preliminary results on another crystal show an increase in the maximum effect from 17:1 at 9.4 kMc/sec to 58:1 at 36 kMc/sec. This increase is less than the increase in ν_e but is at least partly explained by incomplete saturation of the resonance at the higher frequency. The nuclear resonance spectrometer would not operate above 25 Mc/sec and so we were unable to observe the increase in the F^{19} resonance. If we assume that this is also 58:1, then at the temperature 1.4°K of this experiment the F^{19} polarization exceeded 10% in a volume of 1/8 cc.

The measurements were made using a specially designed self-oscillating nuclear resonance detector, and we observed no change in the relative enhancement in going from levels well below nuclear saturation to levels well above. The effect depends to some extent on the field modulation amplitude if this approaches the electron line width. The measurements we quote used much smaller sweeps approximately equal to twice the nuclear line width.

The effect increases with increasing F-center concentration. It is absent in pure crystals characterized by a nuclear spin lattice relaxation time T_1 in excess of 45 seconds at room temperature. It is 3:1 in crystals exposed to x-rays but not visibly colored with $T_1 \sim 5$ sec and 17:1 in dark brown crystals.

The results for other materials at microwave frequencies between 8 and 10 kMc/sec and temperatures between 1.2 and 1.6°K are presented in Table I. The variety of materials yielding a measurable effect suggests that this is a very general way of polarizing nuclei. Almost any type of paramagnetic impurity produces an effect, provided only that the principal nuclear spin lattice relaxation process is via the impurities. With the exception of sapphire and cobalticyanide, the results are similar to those in Fig. 3. In these two materials the effects are much more complex. In sapphire, for example, each line of the Al^{27} quadrupole spectrum is en-

Table I. Maximum enhancement of nuclear resonance absorption in several materials.

Material		Nucleus	Enhancement
$Ce_2Mg_3(NO_3)_6 \cdot 24H_2O$	Ce^{+++}	H^1	25:1
$La_2Mg_3(NO_3)_6 \cdot 24H_2O$	5% Ce^{+++} impurity	H^1	60:1
Synthetic sapphire	0.1% Cr^{+++} impurity	Al^{27}	5:1
$K_3Co(CN)_6$	2.5% ferric impurity	Co^{59}	2:1
Polytetrafluorethylene	Centers due to electron bombardment	F^{19}	38:1
CaF_2	0.01% Ce^{+++} impurity	F^{19}	2:1
LiF	*F* centers due to x-rays	Li^7F^{19}	17:1
LiF	*F* centers, 36 kMc/sec	Li^7	58:1

hanced or reversed to the same extent but, at a fixed field, on sweeping the microwave frequency from 8 to 10 kMc/sec a series of peaks in the enhancement are seen below 9 kMc/sec and a series of peaks in the reversal at frequencies above. These peaks extend over the whole range 2 kMc/sec of our microwave source.

*Fulbright Research Student.

†English Electric Research Fellow.

[1]Erb, Motchane, and Übersfeld, Compt. rend. 246, 2121 and 3051 (1958).

[2]A. Abragam and W. G. Proctor, Compt. rend. 246, 2253 (1958).

[3]N. W. Lord, Phys. Rev. 105, 756 (1957).

STRAIN-INDUCED CHANGES IN THE SEEBECK COEFFICIENT OF *n*-TYPE GERMANIUM

J. R. Drabble and R. D. Groves

Research Laboratories, The General Electric Company, Limited, Wembley, England

(Received April 29, 1959)

We have measured the strain-induced changes in the Seebeck coefficient of oriented specimens of *n*-type germanium (with carrier concentration 3×10^{14}/cc) at mean temperatures of 82°K and 95.5°K. Large changes parallel to the applied stress were observed on [111] and [110] oriented specimens. The corresponding effects for [100] specimens were negligibly small in comparison, thus indicating that the changes are brought about solely as a consequence of the strain-induced changes in the carrier populations of the different valleys. The effect leads in a fairly direct way to an estimate of the anisotropy of the phonon-drag part of the Seebeck tensor for a single valley.

The theory of elastoresistance under these conditions (Herring and Vogt[1]) leads to expressions for the components of the variation of the conductivity with strain which are functions of the deformation potential constants and of $K(=\mu_\perp/\mu_\parallel)$, the ratio of mobilities perpendicular and parallel to the symmetry axis of a single valley. A closely parallel theory can be set up for the components of the variation with strain of the product of the conductivity and Seebeck tensors. These components involve the same parameters as the elastoresistance components together with another parameter L which it is convenient to define as $Q_\parallel/Q_\perp$, the ratio of the components of the partial Seebeck tensor parallel and perpendicular to the symmetry axis of a valley. The theory is not completely analogous to the theory of elastoresistance because the electronic part of the Seebeck tensor for a single valley changes with the carrier concentration. This change however is just k/e times the relative change in the conductivity of the corresponding valley, and thus the combined effect of such changes is simply related to the total conductivity change.

In view of this analysis, we have measured the relative resistivity changes $(\Delta\rho)/\rho_0$ under conditions of stress and temperature distribution

identical with those used to measure the relative changes in the Seebeck coefficient $(\Delta Q)/Q_0$. A chopper technique was used to eliminate the effect of the temperature gradient on the resistivity measurements. The relation between $(\Delta Q)/Q_0$ and $(\Delta\rho)/\rho_0$ gives directly a simple function of the parameters K and L. A second relation involving K, $Q_{\parallel}$, and $Q_{\perp}$ is obtained from the zero-strain value of the Seebeck coefficient.

We have used the K values given by Goldberg[2] to calculate $Q_{\parallel}$ and $Q_{\perp}$. Subtracting the electronic part of these as estimated from low-field Hall data, we have found the ratio of the components of the phonon-drag Seebeck tensor for a single valley, $Q_{p,\parallel}/Q_{p,\perp}$, to have the value 9.6 ± 0.3 at 82°K and 9.5 ± 0.5 at 95.5°K. These agree very well with the values obtained by Herring et al.[3] from an analysis of thermomagnetic effects. They found a value of 9.6 which was independent of temperature in the range 60°K to 100°K.

---

[1]C. Herring and E. Vogt, Phys. Rev. 101, 944 (1956).
[2]C. Goldberg, Phys. Rev. 109, 331 (1958).
[3]Herring, Geballe, and Kunzler, Phys. Rev. 111, 36 (1958); see also Geballe, Herring, and Kunzler, J. Phys. Chem. Solids 8, 347 (1959), and Herring, Geballe, and Kunzler, Bell System Tech. J. (to be published).

COLOR CENTER FORMATION IN SODIUM CHLORIDE

H. W. Etzel and J. G. Allard
United States Naval Research Laboratory, Washington, D. C.
(Received May 8, 1959)

Recent experimental work in this laboratory on the F-center production in synthetic sodium chloride at room temperature by ionizing radiation has revealed growth curves for synthetic crystals which differ from those obtained for halite. From Fig. 1 it can be seen that the natural crystal from Baden, Germany has a simple growth curve whereas in the synthetic crystals the growth curve is somewhat complicated. In recent publications[1,2] the influence of hydroxyl ions inadvertently introduced into synthetic alkali halide crystals by growth in air, has been noted. It is evident from the figure that as the amount of hydroxyl ion (which is related to the absorption coefficient at 1850 A) is reduced, the growth curves for the synthetic crystals approach that of the natural crystal. If the natural crystal contains any impurities, they are not apparent in the growth curve data.

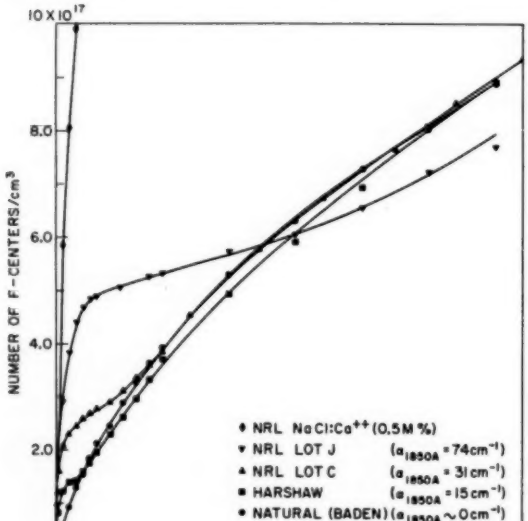

FIG. 1. Growth of the number of F centers produced in NaCl by x-ray radiation as a function of the energy absorbed.

The color center formation in synthetic crystals has been compared to that in natural crystals using 40-kvp x-rays, 2-Mev electrons, and 1.2-Mev γ rays. The flux from these sources has been calibrated and the energy absorbed by the thin crystals ($d = 0.22$ mm) calculated. The number of F centers created per unit absorbed energy agrees within 30% for the 40-kvp x-rays and the 2-Mev electrons where the flux was comparable (6×10^{19} ev/cm²-hr). In the Co^{60} γ-ray exposure, the rate of energy absorption was a factor of 100 less, and the coloration for a given energy absorbed was a factor of 3 lower than that for the other radiations. Despite the low rate of F-center production under γ rays, the shape of the growth curves for the different radiations is the same and the energy initially required to form an F center agrees with that found using x-

rays and high-energy electrons.

In Fig. 1 the growth curves under x-rays are shown for the various specimens. Up to about 10^{20} ev/cm^3 energy absorbed, the rate of coloration varies by as much as a factor of 30 between crystals. It will be noted that the faster-coloring synthetic crystals attain the same color-center concentration and production rate as the natural crystals after prolonged irradiation. This indicates that the entity responsible for the enhanced initial coloration rate in the synthetic crystals is no longer effective for F-center production after prolonged irradiation. This entity is not removed from the crystal, however, because a still higher initial coloration rate is produced if the color centers are optically bleached and the crystal is irradiated again with x-rays. If the entities responsible for the initial enhancement are vacancies, it may be possible that vacancy pairs or higher order complexes are formed under prolonged irradiation which are ineffective for trapping electrons. However, no abnormal growth of the M band or the presence of other higher order bands is observed which can account for the loss of these F centers in synthetic crystals.

In order to facilitate the extrapolation of the data of Fig. 1 to the origin to determine the energy required to form an F center, the data of Fig. 1 are replotted as follows. The abscissa E, the energy absorbed/cm^3, is divided by n, the number of F centers/cm^3, and this ratio is plotted as the ordinate in Fig. 2. The abscissa is the same in both plots. With the exception of the data for the natural crystal, the curves obtained in Fig. 2 are straight lines over a sufficient energy range to be represented by the equation $E/n = mE + b$, where n is the color-center concentration, m is the slope, b is the intercept on the E/n axis, and E is the energy absorbed. The data then indicate that the energy required to form an F center in Harshaw Company NaCl is 96 ev, in NRL NaCl batch C is 85 ev, in NRL NaCl batch J is 73 ev, and in NaCl:Ca is 70 ev. It should be noted that in this plot, the natural crystal data do not give a straight line over any part of the dose range illustrated. By using thick crystals and γ-ray exposures of $(2\text{-}5)\times10^{15}$ ev/cm^2, it has been determined that the energy required to form an F center in the natural crystal is about 85 ev.

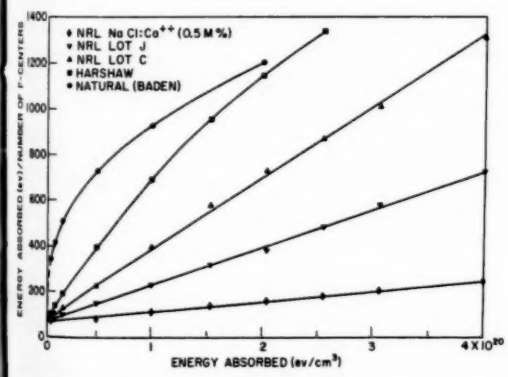

FIG. 2. The x-ray energy absorbed per number of F centers formed in NaCl crystals as a function of energy absorbed.

Despite the wide variation in the rate of color-center production in the various crystals, the energy to form an F center is about the same for all crystals studied although there is some slight variation. This energy is a measure of the efficiency with which an electron in a given crystal is freed from within the lattice and trapped at a negative-ion vacancy to form an F center. The fact that the F-center coloration varies considerably in the mid-range of energy absorbed indicates the presence of a readily available source of vacancies which is dependent upon the crystal history. It is known[2] that air-grown synthetic NaCl has an absorption at 1850 A associated with an hydroxyl ion concentration to which the coloration is proportional. In NaCl doped with calcium, it is known that the irradiation-produced F-center coloration is proportional to the calcium concentration.[3] Preliminary coloration experiments with x-rays on calcium-doped NaCl indicate that the growth curve is well represented by $n = (m + b/E)^{-1}$ to color-center concentrations in excess of 2×10^{18} F centers/cm^3. The fact that the data shown in Fig. 1 are, in the initial rapid-coloring stage, represented by $n = (m + b/E)^{-1}$ in both hydroxyl-bearing and calcium-bearing crystals suggests that a common entity is introduced into these crystals by the impurities. Arguments have been presented for the presence of positive-ion vacancies as being responsible for the enhanced coloration observed in calcium-doped alkali halides.[4] The excess positive-ion vacancies are thought either to aid in the diffusion of negative-ion vacancies from dislocations or to act as traps for holes, reducing the electron-hole recombination. If it is to be assumed that there is an excess positive-ion-vacancy concentration in the hydroxyl-bearing crystals, it would require that the hydroxyl ion substitute for two chlorine

ions in the lattice. Whether this occurs or not could perhaps be verified by measuring the ionic conductivity of a group of crystals having different hydroxyl concentrations.

Finally, it is of interest to note that not only is the energy required to form an F center about the same for these diverse crystals, but for prolonged irradiations the various crystals appear to have the same color-center concentration and rate of production. It would seem then, that the only region in which it would be safe to use the data of synthetic crystals which contain inadvertent impurities for kinetic studies of F-center formation is in the high-dose range where the effects of these impurities are no longer present.

The authors wish to thank Dr. J. H. Schulman, Dr. C. C. Klick, and Dr. H. Rosenstock for many helpful discussions. The authors also express their appreciation to Dr. G. S. Switzer of the Smithsonian Institution for providing the sample of halite from Baden, Germany.

[1]J. Rolfe, Phys. Rev. Lett. 1, 56 (1958).
[2]H. W. Etzel and D. A. Patterson, Phys. Rev. 112, 1112 (1958).
[3]H. W. Etzel, Phys. Rev. 87, 906 (1952).
[4]F. Seitz, Revs. Modern Phys. 26, 7 (1954); see pp. 63, 64.

ELECTRON FREE PRECESSION IN PARAMAGNETIC FREE RADICALS*

D. E. Kaplan and M. E. Browne
Lockheed Research Laboratory, Palo Alto, California
(Received May 11, 1959)

Free magnetic induction signals from the unpaired electron in the organic free radicals, α-α diphenyl-β-picryl hydrazyl, α-γ bisdiphenylene-β-phenylallyl, and picryl-n-amino carbazyl, have been observed. Transverse relaxation times, T_2, in the range 30-100 millimicroseconds were measured directly using pulsed resonance techniques originated by Hahn.[1] Measurements were made on polycrystalline samples at 300°K with an extremely fast time-resolution pulsed spectrometer operating at microwave X-band frequencies (9.3 kMc/sec). Recently, Gordon and Bowers[2] have used pulse methods at 23 kMc/sec to measure T_2's in the range 100-1000 microseconds for paramagnetic resonances in impurity-doped silicon.

A detailed description of the spectrometer used for these measurements will be published later. It utilizes a ferrite circulator and a magnetron which generates 150-watt, 50-millimicrosecond pulses at 9.3 kMc/sec. A terminated TE_{102} transmission cavity ($Q \sim 30$) containing the spin sample in a dc magnetic field is placed in the antenna arm of the circulator. The pulse power and duration produces approximately a 45° pulse in this cavity. One-half of the free precession signal originating in this cavity following a pulse appears in the receiver arm of the circulator and is detected in a broadband superheterodyne system. The output is displayed directly on the plates of a Tektronix 517A oscilloscope.

Figures 1(A), (B), and (C) are oscilloscope photographs of free precession decays following application of a single microwave pulse in the hydrazyl, phenylallyl, and carbazyl radicals, respectively. Samples used contained approximately 10^{20} spins. The first two spikes preceding the spin signal are reflections from leading and trailing edges of the transmitter pulse. The signal minimum occurring shortly following the pulse has been shown by Nelson[3] to arise from dispersion in the angle of rotation of the spin ensemble

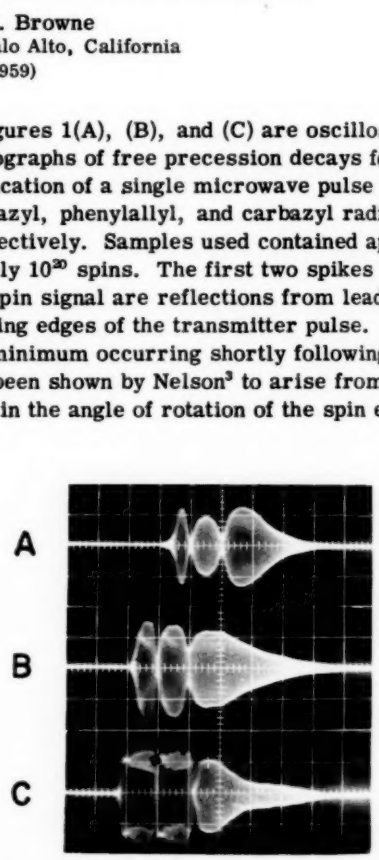

FIG. 1. Free precession signal decay following single pulse in (A) hydrazyl, (B) phenylallyl, and (C) carbazyl. The time scale is 50 millimicroseconds/scale division.

during the pulse on time. The effect is accentuated in this case when the pulse width is not short compared to T_2. The 50-millimicrosecond pulse appears broadened due to receiver overloading. The time constant of the spectrometer at normal signal levels after recovery from saturation is less than 5 millimicroseconds, and hence the signal shape is not distorted. Because the natural line width in these radicals is substantially greater than the dc magnetic field inhomogeneity over the sample volume, T_2 measurements, which were taken directly from the decay envelope, do not reflect external broadening effects.

Lowe and Norberg[4] have shown that the free precession signal decay envelope is closely the Fourier transform of the cw resonance line. The decay envelopes following signal maximum for hydrazyl and phenylallyl were found to be of the form $\exp(-t/T_2)$, implying a Lorentzian cw line in agreement with observations of Bloembergen and Wang,[5] Goldsborough and Mandel,[6] and Lloyd and Pake,[7] that the spin-lattice relaxation time, T_1, equals T_2 in these radicals. The structure of the carbazyl decay envelope reflects the asymmetric line shape reported by Kikuchi and Cohen,[8] and does not permit accurate analysis. Table I compares our results for pulsed measurements of T_2 with those obtained from cw line-width measurements by Pake[9] and Wertz et al.[10] ($\Delta H = 2/\gamma_e T_2$, where $\gamma_e = 1.76\times10^{-7}$ gauss^{-1} sec^{-1} and ΔH is measured between half-intensity points.) The close agreement between cw and pulsed results for hydrazyl and phenylallyl implies that anisotropic broadening, associated with variation of the g factor value with crystalline axis orientation in a magnetic field, is small in these cases. The hydrazyl T_2's are about 30% shorter than values reported by Bloembergen and Wang.[5] The time constant for the long tail of the carbazyl curve is about 100 millimicroseconds, characteristic of the narrow single-crystal line width of 0.5 gauss reported by Kikuchi and Cohen.[8] Because of pronounced anisotropic broadening, the polycrystalline carbazyl line width is about 6 gauss.

Table I. T_2 results at 9.3 kMc/sec.

Free radical (polycrys.)	$(T_2)_{\text{pulsed}}$ mμsec	$(T_2)_{\text{cw}}$ mμsec
hydrazyl	38	41
phenylallyl	83	81
carbazyl	100	110[a]

[a](single crystal).

Spin echoes following application of two successive microwave pulses could not be obtained in these radicals because of short relaxation times and limitations on minimum pulse width for the magnetron. Measurement of T_1 by two-pulse techniques was not possible for similar reasons.

Direct measurement of paramagnetic transverse and thermal relaxation times of less than 1 microsecond in many substances should be possible with this instrument; further, it shows promise of realizing the potentially large information storage capabilities of some paramagnetic systems as demonstrated by Gordon and Bowers.[2]

We wish to thank Professor E. L. Hahn and Professor G. E. Pake for several stimulating discussions. Dr. M. Mandel and Dr. W. Blumberg have contributed valuable suggestions.

---

*Supported in part by the Office of Naval Research.

[1]E. L. Hahn, Phys. Rev. 80, 580 (1950).

[2]J. P. Gordon and K. D. Bowers, Phys. Rev. Lett. 1, 368 (1958).

[3]B. Nelson, "Nuclear Resonance Filters" (final report), TRG, Inc., 1957.

[4]I. J. Lowe and R. E. Norberg, Phys. Rev. 107, 46 (1957).

[5]N. Bloembergen and S. Wang, Phys. Rev. 93, 72 (1954).

[6]J. Goldsborough and M. Mandel (private communication).

[7]J. P. Lloyd and G. E. Pake, Phys. Rev. 92, 1576 (1953).

[8]C. Kikuchi and V. W. Cohen, Phys Rev. 93, 394 (1954).

[9]G. E. Pake (private communication).

[10]Wertz, Koelsch, and Vivo, J. Chem. Phys. 23, 2194 (1955).

OPTICAL AND MAGNETO-OPTICAL ABSORPTION EFFECTS OF GROUP III IMPURITIES IN GERMANIUM*

P. Fisher and H. Y. Fan
Department of Physics, Purdue University, Lafayette, Indiana
(Received May 6, 1959)

The ionization and excitation spectra of Group III impurities in germanium have been measured[1] on single crystals of germanium, held at ~ 5°K, by the use of a far infrared grating spectrometer. Figure 1 shows such a spectrum for boron-doped germanium; this is typical of the Group III impurities. The absorption lines correspond to transitions of bound holes from the ground state of the impurity atom to the various excited states. The energy separations between the absorption lines give a measure of the energy spacings of the excited states. In view of the large dielectric constant of germanium and the small effective masses of its holes, the level scheme of the excited states should be relatively independent of the particular Group III impurity involved.

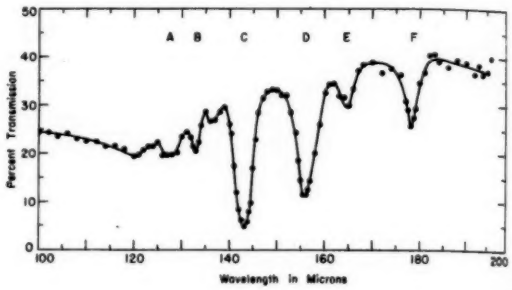

FIG. 1. Transmission spectrum of boron-doped germanium at ~ 5°K. Room temperature resistivity =14 ohm cm. Sample thickness =3.5 mm.

Table I gives the spacings between the various lines and the line D for the four impurities studied. The spacings between the excited states calculated by Schechter[2] are also listed. In comparing the theoretical and experimental values, the strong lines C and D are assigned to the $1s\rightarrow 2p^3$ and $1s\rightarrow 2p^2$ transitions, respectively. The agreement is fair, particularly when one considers the complexity of the theoretical problem. The optical ionization energies are obtained by adding the calculated binding energy of the $2p^3$ state to the energy of line C. These values are in good agreement with the thermal activation energies.

The Zeeman effect on the excitation lines of donor impurities in germanium has been reported previously[3] and satisfactorily explained. This effect has now been studied for an acceptor impurity in germanium. Figure 2 shows the Zeeman pattern of the strong C and D lines of boron impurity for $H \parallel \langle 111 \rangle$. Measurements at different

Table I. Energy level spacings and ionization energies for Group III impurities in germanium, in units of 10^{-3} ev.

	Theoretical[a]		Experimental[b]			
			B	Tl	Ga	In
$2p^4-2p^2$	1.8	A-D	1.76	1.83	1.82	1.72
		B-D[c]	1.36	1.41	1.41	1.37
$2p^3-2p^2$	0.5	C-D[c]	0.71	0.73	0.72	0.73
		D-E	0.43	0.41	0.53	...
$2p^1-2p^2$	1.4	D-F	1.00	1.10	1.19	1.12
		D-G	...	1.69	1.64	1.85
Ionization energies		Optical	10.3	13.0	10.8	11.4
		Thermal	10.4[d]	14[e]	10.8[d]	11.2[d]

[a]See reference 2.
[b]Experimental error is ±0.08 unit for the spacings.
[c]Experimental error is ±0.04 unit.
[d]T. H. Geballe and F. J. Morin, Phys. Rev. 95, 1085 (1954).
[e]M. L. Schultz and G. A. Morton, Proc. Inst. Radio Engrs. 43, 1819 (1955).

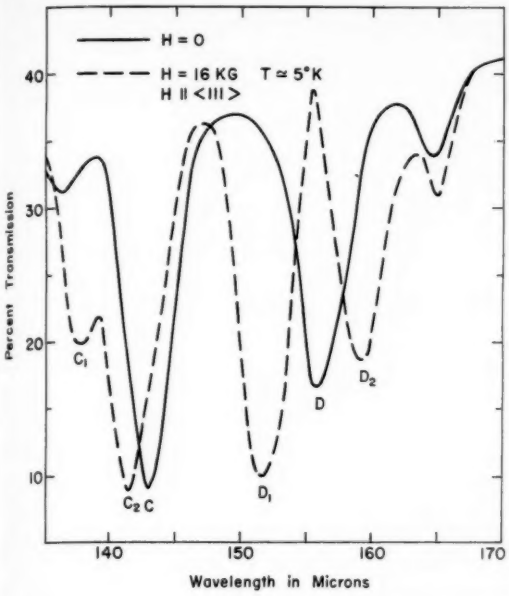

FIG. 2. Effect of a magnetic field on the two strong excitation lines of boron in germanium.

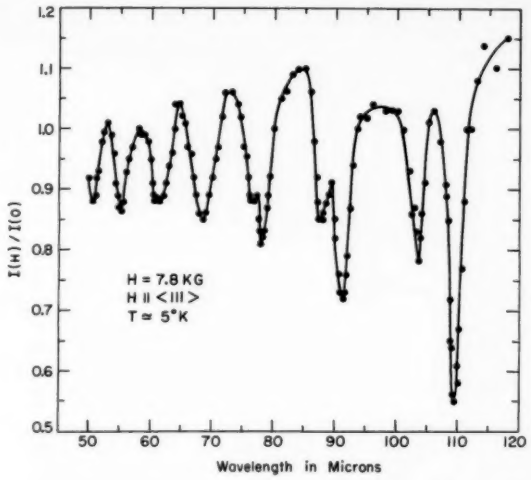

FIG. 3. Effect of a magnetic field on the ionization absorption of boron in germanium. The ordinate is the ratio of transmitted intensity through the sample with and without field.

field strengths show that the splitting of the D line is linear with field (2.5×10^{-8} ev/oersted) with no observable shift in its mean position. The C line appears to be split into two lines, the splitting, however, being only about half that seen for the D line. The C line exhibits a shift of its mean position to higher energies; this shift appears to be a quadratic function of field.

Schechter's analysis shows that the $2p^2$ and $2p^3$ states are fourfold and twofold degenerate, respectively. Thus we may expect a difference between the Zeeman patterns of the C and D lines. According to Wallis and Bowlden,[4] Kohn has shown that the degeneracy of the ground state is lifted in the presence of a magnetic field. However, for the fields used here the expected splitting would be unresolvably small. Even so, it is difficult to understand why the pattern of the D line does not show more multiplicity. A measurement made with $H \parallel \langle 100 \rangle$ gave substantially the same result.

Luttinger's[5] theory for the effect of a magnetic field on the degenerate valence band of germanium predicts two pairs of ladders of energy levels. Roughly, each pair is associated with one of the degenerate bands. Thus the ionization absorption spectrum of a Group III impurity in germanium should show structure under an external magnetic field. Figure 3 shows this effect for boron-doped germanium. The pattern appears to consist of two series of peaks, one series being weaker than the other. Only three of the weak peaks are resolved. Better resolution has been obtained at higher fields. The absorption peaks may be identified with transitions from the impurity ground state to the two light-hole ladders.

The difference between the energy of the first peak in each series and the ionization energy for $H=0$ (see Table I) is 11.0 and 18.3, in units of $(e\hbar/mc)H$. Comparing these values with the theoretically estimated levels[6] in the two light-hole ladders, one can identify the first peak in each series with the level for which $n=1$, where n is the quantum number defining the levels in a ladder and takes the values 0, 1, 2, 3, ... etc. The observed energy spacings between the successive peaks is approximately uniform, 24.8 units in the first series and 23.4 units in the second series. The theoretically estimated spacing is ~23 units for both ladders, provided $n>2$, which is in fairly good agreement with either of the two experimental values. However, within the ladder which has been associated with the first series of peaks the estimated spacing between the levels for $n=1$ and $n=2$ is ~19 units. This value is appreciably smaller than the spacing between the first two peaks in the first series.

*Work supported by the Office of Naval Research.

[1] P. Fisher and H. Y. Fan, Bull. Am. Phys. Soc.

Ser. II, 4, 145 (1959).
[2]Reported by W. Kohn, in Solid-State Physics, edited by F. Seitz and D. Turnbull (Academic Press, New York, 1957), Vol. 5. p. 257.
[3]H. Y. Fan and P. Fisher, J. Phys. Chem. Solids 8, 270 (1959); W. S. Boyle, J. Phys. Chem. Solids 8, 321 (1959).
[4]R. F. Wallis and H. J. Bowlden, J. Phys. Chem. Solids 8, 318 (1959).
[5]J. M. Luttinger, Phys. Rev. 102, 1030 (1956).
[6]Values of the constants used for this calculation are $\gamma_1 = 13.2$, $\gamma_2 = 4.4$, $\gamma_3 = 5.4$, and $\kappa = 4.0$; this last value is estimated from Kohn's value for K (see reference 5). The calculation is made for $H \parallel \langle 111 \rangle$.

RANGE OF ORDER OF SUPERCONDUCTING ELECTRONS*

Hans Meissner
The Johns Hopkins University, Baltimore, Maryland
(Received April 30, 1959)

In the following it is proved that just as superconducting electrons can drift into an adjoining normal conducting layer and make it superconducting, normal electrons can drift into an adjoining superconducting layer and prevent superconductivity.

It has been found earlier that an interposed normal conducting barrier does not necessarily prevent the superconductivity of a contact between two superconducting wires.[1] This has been explained by the assumption that the density of the superconducting electrons in the normal conducting barrier decreases relatively slowly with distance from the superconductor. Observations of the barrier thickness at which superconductivity disappears therefore provide an estimate of the "range of order" of the superconducting electrons. The following thicknesses in 10^{-6} cm have been observed for the metals listed:

Group	I*B*	VI*A*	VIII		
Metal	Cu: 30	Cr: 4	Fe: 0.7	Co: 2	Ni: 1.0
	Ag: 40	...	...	...	...
	Au: 35	...	...	...	Pt: 7.5.

The lower values of the thicknesses observed for the ferromagnetic barriers may be caused by quenching of superconductivity in the neighborhood of the contact due to the high magnetic fields emerging from the barrier layers.

The experiments have been extended to measurements of the contact resistance (transverse resistance) and the resistance along the wire (longitudinal resistance) of normal conducting wires plated with tin. While it is known[2] that films of tin evaporated onto glass are superconducting at thicknesses as low as 1.6×10^{-6} cm, it has been observed that films of tin electroplated onto gold wire do not become superconducting if their thickness is less than 60×10^{-6} cm. Similar measurements of tin plated onto copper wire showed that these do not become superconducting below 20 $\times 10^{-6}$ cm.

These observations confirm early measurements by Burton, Wilhelm, and Misener[3] on tin, and by Misener and Wilhelm[4] on lead. These and subsequent measurements by Misener[5] were usually believed to be unreliable (see the remark by Feigin and Shal'nikov[6] and by Shoenberg[7]), because they disagreed with the measurements of superconducting films evaporated onto glass or quartz surfaces. Since in the present experiments the time between plating and measurement in liquid helium was less than 2 hours, it is unlikely that the results are falsified by alloying or diffusion. It is much more likely that just as the superconducting electrons "spill over" into the normal conducting barriers, also the normal conducting electrons of the base metal can prevent superconductivity of the film. This effect is to be expected in view of the recent treatment of "dirty" superconductors by Anderson.[8]

The measurements of the contact resistance represent in a way the "transverse" resistance of the film. Their results are very similar to those observed on contacts between normal-conducting and superconducting wires.[9] At lower temperatures the resistance disappears partially, but is, at least for the thinner films, still measurable even at 5 μa and 1.48°K. A decrease in transverse resistance is observed already for films thin enough that the longitudinal resistance is almost independent of current and temperature.

It is planned to repeat the experiments by simultaneous evaporation of tin onto glass and metal

rods and comparison of the I-T diagrams for various film thicknesses.

---

*Work supported by a contract with the Office of Naval Research.

[1]Hans Meissner, Phys. Rev. 109, 686 (1958).
[2]N. E. Alekseyevsky, J. Phys. U.S.S.R. 4, 401 (1941).
[3]Burton, Wilhelm, and Misener, Trans. Roy. Soc. Can. 28, Sec. III, 65 (1934).
[4]A. D. Misener and O. Wilhelm, Trans. Roy. Soc. Can. 29, Sec. III, 5 (1935); also Univ. Toronto Studies 72, 12 (1935).
[5]A. D. Misener, Can. J. Research 14, 25 (1936).
[6]L. A. Feigin and A. I. Shal'nikov, Doklady Akad. Nauk. U.S.S.R. 108, 823 (1956)[translation: Soviet Phys. Doklady 1, 377 (1957)].
[7]D. Shoenberg, Superconductivity (Cambridge University Press, Cambridge, 1952). See note at bottom of p. 166.
[8]P. W. Anderson, J. Phys. Chem. Solids (to be published).
[9]F. Bedard and H. Meissner, Phys. Rev. 101, 26 (1956).

OBSERVATION OF THE Co^{59} NUCLEAR MAGNETIC RESONANCE IN PARAMAGNETIC SALTS

R. G. Shulman
Bell Telephone Laboratories, Murray Hill, New Jersey
(Received April 29, 1959)

Moriya[1] has considered theoretically the possibility of observing the nuclear magnetic resonance (NMR) signal from the nuclei of magnetic ions in the paramagnetic state. He pointed out that the resonance in the iron group would be affected by the strong internal magnetic fields (10^5-10^6 gauss). In dense magnetic materials, rapid fluctuations of the electron spins by the exchange interaction will result in "exchange-narrowed" nuclear resonance lines which calculations indicated might be observable. It has been shown[2] that the F^{19} resonance in paramagnetic MnF_2 is affected in just these ways by hyperfine interactions with the magnetic electrons. Internal fields at the F^{19} nuclei are about one order of magnitude smaller than those at the magnetic ion nuclei. By choosing a material where the exchange frequency is large and the hyperfine fields reasonably small, one increases the possibility of observing the resonance. In addition, since all the iron group elements which have magnetic moments also have large quadrupole moments, it is desirable to pick a salt where the magnetic ion is in a cubic environment. $KCoF_3$ and CoO with Néel temperatures of 137°K and 293°K, respectively, both with cubic structures, the former being perovskite and the latter NaCl, were considered suitable substances in which to search for the Co^{59} resonance.

We have been able to observe the Co^{59} resonance in both substances and shall consider the $KCo^{59}F_3$ results in detail. In Fig. 1 a recorder plot of the derivative of the $KCo^{59}F_3$ resonance at 298°K is presented. It was taken with a Varian Associates Variable Frequency NMR spectrometer adjusted for maximum H_1. The solid line is a calculated derivative curve for a Lorentzian line on the assumption that $T_2 = 1.43 \times 10^{-6}$ second. The line shape is seen to be Lorentzian as would be expected for an exchange-narrowed line. At 298°K the center of the resonance corresponded

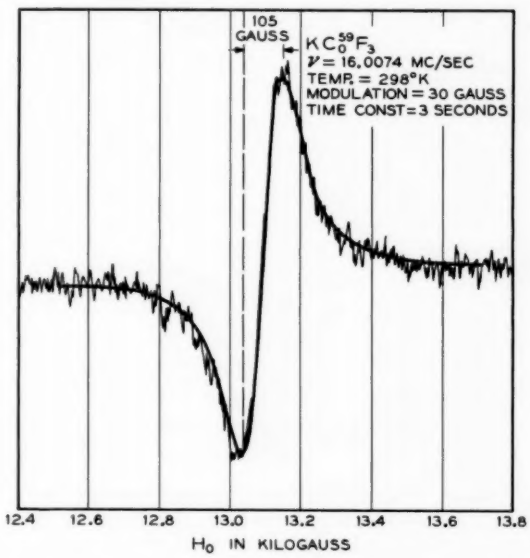

FIG. 1. Copy of recorder trace of the derivative of $KCo^{59}F_3$ absorption. The solid curve is calculated for a Lorentzian line shape.

to $g_{eff}=\gamma_{eff}/2\pi=1.2232\pm0.0002$ (kc/sec)/gauss. The effective g value for Co^{59} has been measured by NMR in diamagnetic compounds[3] and in the antiferromagnetic state.[4] It has been shown to have different values between 1.01 and 1.25 (kc/sec)/gauss. This variation has been explained[5,6] by considering the contributions of low-lying excited states to the chemical shift and hyperfine interactions. Presumably these mechanisms are responsible for the g value observed in our compounds. The effective g value was measured between 195°K and 368°K and it is plotted vs temperature in Fig. 2. At 195°K the line was narrower than at 298°K, and it was determined that $T_2=1.87\times10^{-6}$ second at 195°K.

The salient features of the phenomena responsible for the line shapes, widths, and g factors are as follows. At the Co^{59} nuclei there are large time-dependent magnetic fields[7] from both the spin and orbital moments of the magnetic electrons. In a cubic crystal field, the ^4F ground state of the Co^{++} ion is split into two orbital triplets and one singlet, with a twelve-fold degenerate orbital triplet lowest. Under the influence of the spin-orbit interaction, the lowest triplet is split so that the lowest level is a Kramers doublet separated by ~400 cm^{-1} from the first excited state which is fourfold degenerate. We assume, therefore, that to a first approximation we can evaluate the interaction in the ground-state doublet ignoring the mixing with excited states. Furthermore, since this is several times the magnetic exchange energy, we assume that both spin and orbital interactions are exchange-narrowed with the same correlation time $\omega_e=7\times10^{12}$ $second^{-1}$ as estimated from the molecular field approximation.

The nuclear Hamiltonian given by Abragram and Pryce[7] for the lowest doublet is

$$W_n=-\gamma_n\hbar\vec{I}\cdot\vec{H}+P\vec{I}\cdot\vec{N},$$

where

$$\vec{N}=\vec{L}+(1/105)\{\vec{L}(\vec{L}\cdot\vec{S})+(\vec{L}\cdot\vec{S})\vec{L}\}-[(8/105)+\kappa]\vec{S},$$

$$\kappa=\frac{8\pi}{3}\frac{|\psi(0)|^2}{\langle 1/r^3\rangle},$$

$$P=2\gamma_n\mu_B\hbar\langle 1/r^3\rangle. \quad (1)$$

For Co^{++} it has been shown[8] that $P=22\times10^{-3}$ cm^{-1} and $\kappa=0.32$. From these values we calculate that $\langle N^2\rangle=0.13$. It is possible to provide an experimental comparison with this value by using a model of Gaussian random modulations to obtain[9]

$$1/T_2=(\tfrac{1}{2}\pi)^{1/2}P^2\langle N^2\rangle/(2\hbar^2\omega_e). \quad (2)$$

Substituting the above values for P^2, ω_e, and T_2, we find that $\langle N^2\rangle=0.23$. Considering the assumptions mentioned above, this agreement with the calculated value lies within reasonable expectations. Additional experiments to separate the temperature-independent and temperature-dependent effects are underway.

With F. J. Morin we have observed the Co^{59} resonance in CoO in the paramagnetic state. At 298°K, $g_{eff}=1.2012\pm0.0002$ (kc/sec)/gauss while $T_2=(1.16\pm0.1)\times10^{-6}$ second.

It is a pleasure to thank Dr. K. Knox who called the interesting properties of $KCoF_3$ to our attention and who supplied the powdered samples used, Dr. T. Moriya for enlightening discussions of these results, and Mr. B. J. Wyluda who helped with the experiments.

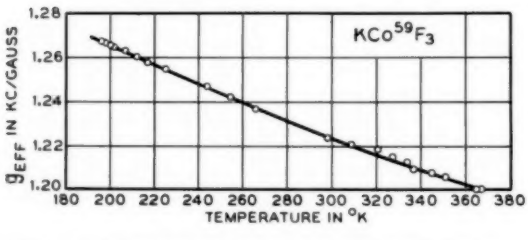

FIG. 2. Experimental value of g_{eff} vs temperature. When susceptibility measurements are made and interpreted, the functional form of the temperature-dependent part of the NMR shift will be known. It will then be possible to separate the temperature-dependent component of the shift from the temperature-independent component by extrapolating to infinite temperature.

[1]T. Moriya, Progr. Theoret. Phys. (Kyoto) 16, 641 (1956).
[2]R. G. Shulman and V. Jaccarino, Phys. Rev. 108, 1219 (1957).
[3]W. G. Proctor and F. C. Yu, Phys. Rev. 81, 20 (1951).
[4]V. Jaccarino, Phys. Rev. Lett. 2, 165 (1959).
[5]J. S. Griffith and L. E. Orgel, Trans. Faraday Soc. 53, 601 (1957).
[6]T. Moriya (to be published).
[7]A. Abragram and M. H. L. Pryce, Proc. Roy. Soc. (London) A205, 135 (1951).
[8]B. Bleaney and D. J. E. Ingram, Proc. Roy. Soc. (London) A208, 143 (1951).
[9]T. Moriya (private communication).

PLASMA PINCH EFFECTS IN INDIUM ANTIMONIDE

M. Glicksman and M. C. Steele
RCA Laboratories, Princeton, New Jersey
(Received May 11, 1959)

In pulsed studies of the properties of n-type indium antimonide at 77°K in high electric fields, some interesting effects were observed in the presence of an external longitudinal magnetic field.[1] It is now suggested that these observations indicate the presence of pinching effects for the electron-hole pair current in indium antimonide. It is believed that this represents the first published indication of the existence of pinch effects in a solid. Of course the pinch effect in gaseous plasmas[2] is well known.

Measurements were made on two samples with an electron density of 2×10^{14} cm^{-3} at low electric fields. The single crystal used for the observations shown in Fig. 1 was rectangular in cross section, 0.39 mm × 0.60 mm, and about 8 mm long. The voltage was measured between two cross arms which were part of the crystal, spaced 2.5 mm apart. The pulse length of 1 μsec and repetition rate of 1 cps were chosen to minimize heating effects. Data obtained from the two samples agreed well within the precision of measurement, which was about 3%.

The pertinent results are shown in detail in Fig. 1, in which the measured current is plotted as a function of voltage for three cases: (1) with no external magnetic field, (2) with an applied longitudinal magnetic field of 350 gauss, and (3) with an applied longitudinal magnetic field of 3500 gauss. In the first case, it is seen that at low voltages the current is ohmic, dropping off to lower than ohmic slope for voltages greater than several volts. At voltages above about 20 volts there is a change in behavior, with the current rising more steeply than before, and the slope continually increasing to the highest voltages observed. This general increase is due to electron-hole pair creation in the crystal.[1,3] Curve (2) follows the same values until a current of 5 amperes, at which point it abruptly begins to rise sharply with a slope greater than that of curve (1). However, for currents of 13 to 20 amperes, curve (2) approaches curve (1) and for currents larger than 20 amperes the curves are again coincident.

Curve (3) is somewhat displaced from the other two at low voltages, indicating a higher resistance. Since it is expected that there is no longitudinal magnetoresistance at low voltages, this is ascribed to the geometry used (samples with arms) which involves some disturbance of the current lines at the side contacts so that the magnetic field is not parallel to the current in this region. The effect observed is only about 5% of that observed in the same transverse magnetic field.[3] It is noted for curve (3) that the current rises very steeply at voltages of the order of 60 volts and continues in this rise to the highest currents obtained.

It is clear that the curves in a longitudinal magnetic field rise more steeply than does the curve with no external magnetic field. These sharper-rising curves are believed proportional to the current density j as a function of electric field. Curve (1) rises less steeply, however, because for currents larger than 5 amperes the current

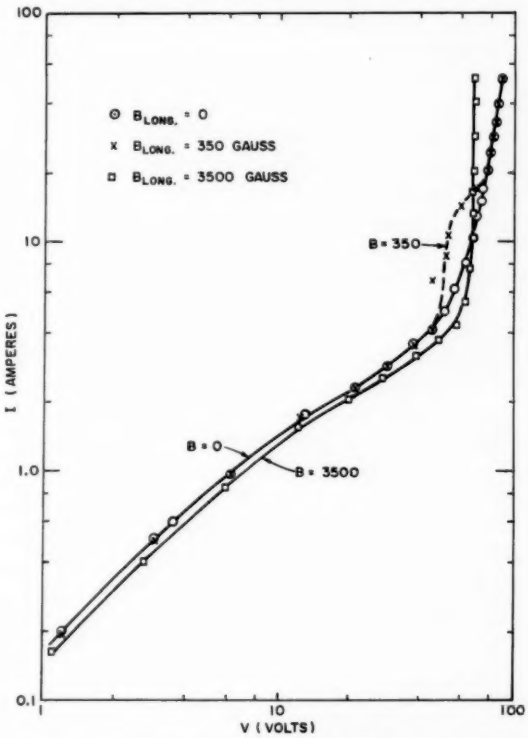

FIG. 1. Current as a function of voltage for n-type indium antimonide at 77°K. The current and the magnetic field were in the [100] direction.

due to the electron-hole pairs is pinched down by the self-magnetic field: this electron-hole current occupies a geometrical space effectively much smaller than the cross section of the sample. This curve is not then proportional to the current density, but should be stretched in the direction of increasing ordinate to yield such a proportionality, i.e., the I-V curve is less steep than the j-V curve. Where the pinch becomes very small, the density will become large enough to give appreciable electron-hole scattering. In addition, there will be an appreciable magnetoresistance effect due to the large azimuthal magnetic field. Both of these effects will increase the electric field necessary to produce a given current density, adding to the slowness of rise of curve (1).

With the application of a longitudinal magnetic field, the pinched plasma should be affected in two ways. In the first place it will be enlarged. The equilibrium diameter of a pinched plasma in a gas is larger in an external longitudinal magnetic field,[4] and when the field is about equal to the azimuthal current-produced magnetic field[4,5] the pinch is effectively destroyed. In addition, there is an improvement in the stability of the pinch of gaseous plasmas in an external longitudinal magnetic field.[4,6,7]

The effect of the magnetic field can be seen from the behavior of the curves in Fig. 1. At 5 amperes pinching sets in, in the absence of a longitudinal magnetic field. For both curves (2) and (3) there is no pinching at this current, however. For curve (2), when the current becomes so large that the azimuthal self-magnetic field approaches the strength of the external magnetic field, the current does pinch down, reaching an equilibrium similar to that without the external field for currents of 20 amperes and higher. For curve (3), with an external longitudinal field of 3500 gauss, the azimuthal self-field is too small over the range investigated to give pinching.

The pinched plasma current in the solid can be treated in a way similar to the situation in the gas.[2,8,9] Such a treatment yields the following condition for a "steady state" pinched plasma with no applied magnetic field:

$$I \approx I_{cr} = 2ck(T_e + T_h)/ev,$$

where k is Boltzmann's constant, T_e and T_h are the mean kinetic temperature of the electrons and holes in the plasma current, v is the electron drift velocity, and I is the current in electromagnetic units. When I approaches I_{cr}, appreciable pinching will occur. The drift velocity is known from previous work.[1,3] The sum of the electron and hole mean energies, at a current of about 5 amperes, is then found to be 0.13 ev. This value is reasonable, indicating that the average energy is larger than the optical phonon energy[10] of 0.025 ev, but less than the band gap of about 0.2 ev. In the 350-gauss longitudinal magnetic field, currents of 10 to 15 amperes correspond to self-magnetic fields at the sample surface of 110 to 165 gauss. This is apparently sufficient to initiate pinching, in qualitative agreement with the gaseous plasma results observed by Bezbatchenko and co-workers.[4]

It is expected that the size of the pinch, in the absence of the longitudinal magnetic field, will be limited by a balance between the supply of electron-hole pairs and the loss through diffusion and recombination outside the pinch. For small external longitudinal fields, this may still be the dominant effect, since curves (1) and (2) are coincident at currents of 20 amperes and higher.

The current in the presence of external transverse magnetic fields will also be affected by the pinching, with the expectation that the plasma current will be forced to one side of the crystal by the external field. Calculations of the plasma current in the presence of external magnetic fields are in progress.

The question of the stability of such a pinched discharge is worth further exploration. The experiments involved pulses of 1 μsec duration, with a rise time of the order of 0.1-0.2 μsec. Estimates of the time of contraction, using the theoretical results of Leontovich and Osovets[11] for a gaseous plasma, yield about 0.01 μsec. This treatment ignores collisions, and thus gives a lower limit for this time. A simple estimate which includes the effects of scattering yields about 0.1 μsec for the crystal used. This time is much longer in InAs, and somewhat longer (because of the lower hole mobility) in the p-type InSb used in previous work.[12] It may be for this reason that similar effects were not observed at currents of 100 amperes in InAs,[13] or the p-type InSb. In both of these materials the I-V curve was much steeper than that observed in n-type InSb in the absence of a longitudinal magnetic field, in agreement with the expectation that no pinching occurred during those observations.

The period of quasi-stability of the pinch must have been at least of the order of 1 μsec, since there was no sign of changing currents during

the pulse. It should be noted that the observing oscilloscope would not have noted any oscillations in the current or voltage at frequencies above several megacycles per second.

We should like to thank M. A. Lampert and Dr. L. S. Nergaard for many helpful discussions of plasma effects in solids.

[1]M. C. Steele and M. Glicksman, J. Phys. Chem. Solids 8, 242 (1959).
[2]W. Bennett, Phys. Rev. 45, 890 (1934).
[3]M. Glicksman and M. C. Steele, Phys. Rev. 110, 1204 (1958).
[4]Bezbatchenko, Golovin, Ivanov, Kirillov, and Iavlishkii, Doklady Akad. Nauk S.S.S.R. 111, 319 (1956) [translation: Soviet Phys. Doklady 1, 640 (1957)].
[5]Butt, Carruthers, Mitchell, Pease, Thonemann, Bird, Blears, and Hartill, Proceedings of the Second United Nations International Conference on the Peaceful Uses of Atomic Energy (United Nations, Geneva, 1958), Vol. 32, p. 42.
[6]M. Kruskal and J. L. Tuck, Proc. Roy. Soc. (London) A245, 222 (1958).
[7]M. Rosenbluth, Los Alamos Scientific Laboratory Report LA-2030 (unpublished).
[8]L. Tonks, Phys. Rev. 56, 360 (1939).
[9]P. C. Thonemann and W. T. Cowhig, Proc. Phys. Soc. (London) B64, 345 (1951).
[10]H. Ehrenreich, J. Phys. Chem. Solids 2, 131 (1957).
[11]M. A. Leontovich and S. M. Osovets, Atomnaya Energ. 1, No. 3, 81 (1956)[translation: Soviet J. Atomic Energy 1, 371 (1956).
[12]M. C. Steele and M. Glicksman, Bull. Am. Phys. Soc. Ser. II, 3, 377 (1958).
[13]M. C. Steele, Bull. Am. Phys. Soc. Ser. II, 4, 28 (1959).

MULTIPLET STRUCTURE OF EXCITONS IN CdS*

R. G. Wheeler
Sloane Physics Laboratory, Yale University, New Haven, Connecticut
(Received May 8, 1959)

A band model has been proposed recently by a number of authors[1,2] to explain the optical reflection and luminescence excitation spectra of CdS,[3,4] wurtzite structure. The model assumes a p-like valence band and an s-like conduction band with the extrema at $\vec{k}=(0,0,0)$, in the reduced zone. The p-like valence band is split by the crystal-field and spin-orbit effects into three bands. Using these assumptions, optical selection rules may be derived from the symmetry properties associated with the bands. The individual bands may be tentatively assigned by interpreting the polarization effects observed in the experiments with use of the selection rules. The assignment of the extrema to be at $\vec{k}=(0,0,0)$ is not unique since other symmetry points of the zone have group properties, as far as the selection rules are concerned, isomorphic with those at $\vec{k}=(0,0,0)$. In terms of the model, the extrema at $\vec{k}=(0,0,0)$, Fig. 1, indicate the energy splittings and the symmetry assignments as deduced from experiments in this laboratory[5] as well as elsewhere.[3,4] The upper valence band symmetry assignment of Γ_9 is indicated by the fact that at 4.2°K the edge luminescence is completely polarized perpendicular to the c axis.

This note is to report on the line absorption spectra near the absorption edge of CdS single crystals at 4.2°K and on the possible interpretation using this model. The absorption spectra were taken of single crystal platelets grown by the vapor phase sublimation method. The samples used were free of visible streaking often observed in platelets of this material. Further, the samples were not subject to any kind of surface preparation, such as polishing, etching, or cleavage. Since the c axis of the crystal lay in the plane of the platelet, orientation was easily

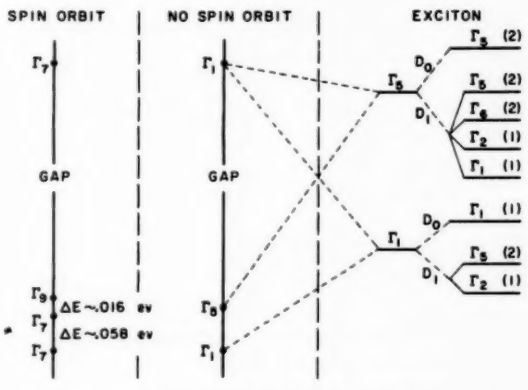

FIG. 1. Band structure at $\vec{k}=(0,0,0)$ of wurtzite CdS, and the possible exciton levels when spin-spin interactions are included.

accomplished by using light incident normal to the plane of the platelet, whereupon the location of the c axis was obtained using the birefringent property of hexagonal crystals. The crystal thicknesses were determined either with a microscope or by interference patterns.

The spectrograph used to observe the spectra was a large Hilger Littrow mounting with glass optics, providing a dispersion of about 9 A/mm, with a resolution for emission lines of about 0.4 A.

In considering these spectra, as pointed out by Gross,[6] some lines are variable from crystal to crystal, especially if individual crystals are subjected to surface deterioration or prolonged heat treatment. Thus, if one considers only the indicated lines of Fig. 2 (numbered 1-5) which appear in all spectra, or are not present due to progression to thinner samples, one observes 5 sharp lines in the region between 4890 A and 4850 A.

One may arrive at a possible interpretation of these lines by considering them all as possible ground-state excitons originating from the Γ_5 valence level. Initially, consider the valence band split by the crystal field into the twofold degenerate Γ_5 band and the nondegenerate Γ_1 band. Assuming the conduction band has a Γ_1 symmetry, any excitons formed of the two states have the symmetry of the direct product of the valence and conduction band symmetries. This means, of course, that the symmetry of the exciton band will be Γ_5. Now suppose we include spin-spin interaction between the hole and the electron making up the exciton. This means that we generate triplet and singlet states by forming the direct product of Γ_5 with D_0 (singlet) and D_1 (triplet). Here in the irreducible representations of the hexagonal group C_{6v},[7,8] D_0 transforms as Γ_1, and D_1 transforms as $\Gamma_2+\Gamma_5$. Thus we are led to the levels indicated in Fig. 1. As has been pointed out by Overhauser,[8] if the spin-orbit splitting of such a p-like valence band is of the same magnitude as the exciton Coulomb and exchange energies, the selection rules prohibiting transitions to "triplet" states are relaxed. In fact, the transition probabilities may be significant. Thus we should like to suggest that the five indicated lines should be ascribed to the ground states of different terms in the exciton spectra. This interpretation may be further borne out by the Zeeman splitting of CdS lines indicated in photographs published by Gross.[9] The degeneracies, indicated in Fig. 2, of the exciton levels show that upon splitting by a magnetic field, the lines will either be split into only two components or not at all. Although Gross's photograph indicates that the line at 4857 A is split into two components, unfortunately his plate does not cover the necessary spectral range nor is the magnetic field orientation and polarization of the light given. Thus, due to the group-theoretical selection rules, an unequivocal interpretation cannot be made with relation to the magnetic line splittings observed by Gross.

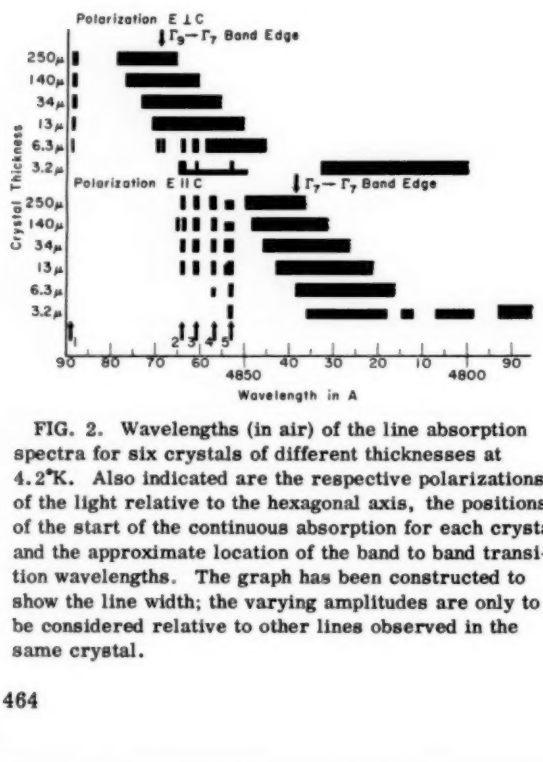

FIG. 2. Wavelengths (in air) of the line absorption spectra for six crystals of different thicknesses at 4.2°K. Also indicated are the respective polarizations of the light relative to the hexagonal axis, the positions of the start of the continuous absorption for each crystal, and the approximate location of the band to band transition wavelengths. The graph has been constructed to show the line width; the varying amplitudes are only to be considered relative to other lines observed in the same crystal.

The lines at wavelengths shorter than 4840 A probably are exciton levels due to transitions from the Γ_1 valence band. In this case the observed lines probably do not involve triplets because of the absence of the spin-orbit mechanism to relax the optical selection rules. More probably the lines are analogous to the hydrogenic excitons observed in Cu_2O, deviations from the Balmer-like spectra due to nonspherical energy bands.[10]

It is a pleasure to thank Dr. P. B. Dorain and Dr. J. L. Birman for helpful discussions as well as Dr. D. C. Reynolds for the supply of crystals.

---

*This research was supported in part by the U. S. Air Force through the Air Force Office of Scientific Research of the Air Research and Development Command.

[1]J. Hopfield, Bull. Am. Phys. Soc. Ser. II, 3, 409

(1958), and J. Phys. Chem. Solids (to be published).
[2]Joseph L. Birman, Phys. Rev. Lett. 2, 157 (1959), and Phys. Rev. (to be published).
[3]D. Dutton, J. Phys. Chem. Solids 6, 101 (1958), and Phys. Rev. 112, 785 (1958).
[4]D. G. Thomas, Bull. Am. Phys. Soc. Ser. II, 4, 154 (1959).
[5]R. G. Wheeler and P. B. Dorain (to be published).
[6]E. F. Gross and B. S. Razbirin, J. Tech. Phys. U.S.S.R. 27, 2173 (1957)[translation: Soviet Phys. (Tech. Phys.) 2, 2014 (1957)].
[7]G. Dresselhaus, Phys. Rev. 105, 135 (1957).
[8]A. W. Overhauser, Phys. Rev. 101, 1702 (1956).
[9]E. F. Gross, J. Phys. Chem. Solids 8, 172 (1959).
[10]G. Dresselhaus, J. Phys. Chem. Solids 1, 14 (1956).

FERRIMAGNETIC RESONANCE LINE WIDTHS AND g-FACTORS IN FERRITES

Robert L. White
Hughes Research Laboratories, Culver City, California
(Received May 7, 1959)

A theory of resonance g-factors[1] and line widths[2] for the rare earth garnets which gives reasonable agreement with all available experimental data has recently been developed by Kittel, Portis, and de Gennes. The purpose of this Letter is to extend the above theory to other magnetic systems, in particular the spinel-type ferrites.

The KPdeG theory hinges on the demonstration that (1) a lattice of ions (the rare earths) exhibiting a relaxation frequency high compared to all other frequencies involved in the motion will contribute a precessing magnetization to the system but essentially no coherently precessing angular momentum, and (2) an ion of very high relaxation frequency, exchange-coupled to a precessing low-loss magnetic system, will effectively scatter energy out of a uniform precession and into shorter spin waves.

The extension of the theory rests upon two further observations: (1) that the rapidly relaxing ions need not be sequestered onto a distinct sublattice to exhibit the properties cited above, and (2) that certain ions of very short relaxation time do indeed commonly occur in ferrites.

Any of the transition elements whose lowest lying state in an octahedrally or tetrahedrally coordinated site of cubic symmetry is not an orbital singlet is a candidate for the role played by the rare earth ions in the rare earth garnets. In particular, Fe^{2+}, Co^{2+}, and Mn^{3+} in octahedrally coordinated sites and Fe^{2+}, Ni^{2+}, or Mn^{3+} in tetrahedrally coordinated sites will possess such energy levels, since these ions will then have ground states which are orbital doublets or triplets split only by spin-orbit interaction or crystal field components of lower symmetry. Fe^{2+}, most likely the principal source of line width in ferrites generally, has been observed in the paramagnetic state[3] to have a short relaxation time T_1 even at reduced temperatures ($T_1 = 5\times10^{-9}$ sec at 20°K, $T_1 = 10^{-10}$ sec at 80°K). As pointed out by KPdeG, the relaxation time T_1 is theoretically inversely proportional[4] to H^2 and may be further greatly shortened by the enhancement of the applied field by the exchange fields; i.e., T_1 may be several orders of magnitude shorter in the ferrites than in a diamagnetic host.

Several general features of the available data on ferrites tend to confirm the hypothesis that the KPdeG relaxation process is a dominant one in these materials:

1. Magnetite, Fe_3O_4, which certainly contains Fe^{2+} ions, shows a very wide (2000-3000 gauss) resonance line.

2. Yttrium iron garnet, which should contain exclusively Fe^{3+} ions (ground state, orbital singlet) and essentially no Fe^{2+} ions, shows exceedingly narrow ($\Delta H < 0.5$ gauss) resonance lines.

3. A maximum in line width as a function of temperature is observed in iron-rich manganese and manganese-zinc ferrites. This maximum is characteristic of motionally narrowed resonances and is expected in this case when the relaxation frequency of the spin scattering ion becomes commensurate with the precession frequency of the system.

4. The addition of small amounts of Zn^{2+}, unambiguously divalent, to iron-rich manganese ferrite greatly reduces the observed resonance line width. It is suggested that divalent zinc reduces the concentration of divalent iron.

5. A high degree of correlation exists between large magnetic anisotropy and large resonance line widths (single crystal) in the ferrites. In the present theory the same low-lying energy levels which give rise to magnetic anisotropy[5] tend to

give rise also to short relaxation times, and the correlation is expected.

It is also possible that the resonance g-factors observed in the ferrites can be understood on the basis of the momentum-quenched ions. If, for instance, the Fe^{2+} ions occur preponderantly on the octahedral sites, the quenching of their angular momentum will cause the net effective g-factor to be raised, in accord with the experimental observation that the g-factors for the ferrites are usually somewhat greater than one would expect. It is probable, however, that the above argument on the g-factors should for the present be regarded with some suspicion inasmuch as ad hoc assumptions concerning ion distributions are being invoked.

The author is indebted to his colleagues and especially to C. Kittel for discussions illuminating the subject of magnetic relaxation, and to C. Kittel, A. M. Portis, and P. G. de Gennes for making available the results of their theory prior to publication.

[1]C. Kittel, Phys. Rev. (to be published).
[2]Kittel, Portis, and de Gennes (to be published); hereafter referred to as KPdeG.
[3]M. Tinkham, Proc. Roy. Soc. (London) A236, 535 (1956).
[4]R. de L. Kronig, Physica 6, 33 (1939); J. H. Van Vleck, Phys. Rev. 57, 426 (1940).
[5]W. P. Wolf, Phys. Rev. 108, 1152 (1957); K. Yosida and M. Tachici, Progr. Theoret. Phys. (Kyoto) 17, 331 (1957).

INTERACTIONS OF 1.15-Bev/c K^- MESONS IN EMULSION*

Walter H. Barkas, Nripendra N. Biswas, Donald A. DeLise, John N. Dyer, Harry H. Heckman, and Francis M. Smith
Lawrence Radiation Laboratory, University of California, Berkeley, California
(Received May 13, 1959)

We have exposed a large stack of Ilford K.5 emulsion to the 1.15-Bev/c separated K^- beam developed by Good and Ticho.[1] By area scanning we have located some 600 interactions with emulsion nuclei. This report deals with two groups of data: (A) an unbiased sample of 102 interactions, and (B) a selected group of interactions which produced more than one prong near the minimum of ionization or which gave evidence of strange-particle production in the plate in which the event was located.

The results of this study are as follows: (a) clear evidence for the reactions $K^- + N \to \pi + \pi + Y$ and $K^- + N \to K^- + N + \pi + \pi$; (b) evidence for the reaction $K^- + N + N \to Y + Y + K^0$ or $K^- + N \to \Xi^- + K^0$ followed by $\Xi^- + N \to Y + Y$; (c) a possible case of a "cascade hyperfragment," that is, one which contains two units of negative strangeness; (d) no cascade particle or K^+ meson was definitely identified.

(A) Analysis of an unbiased sample of 102 stars.- The interactions studied in this portion of our analysis include all of the events located in a single pellicle. Based upon the relative populations of $K:\pi:\mu$ in the beam as estimated by Alvarez et al.,[1] we estimate that 93% of these stars were produced by K^- mesons.

In Table I we summarize the salient features of this analysis.

All the particles produced in these interactions were followed until they came to rest (594), or interacted, decayed, or left the emulsion stack (74). In only a few cases were the tracks not suitably oriented for analysis.

It is recognized that area scanning could bias our prong distribution toward large stars. The

Table I. Summary of analysis of 102 stars.

K^-	Prong distribution			Distribution of reaction products						
Bev/c	Mean	Mode	H. F.	$\Sigma^\pm$	2π	1π	$\pi^\pm$	$(K^-)_{\text{inelastic}}$	Stable	π^+/π^-
1.15	6.5	5	7	25	7	35	49	3	584	9/19

observed distribution extended to 15 prongs (1 event) and reached a maximum at 5 prongs (17 events). Only 3 stars of 2 prongs were found, which leads us to believe that 0- and 1-prong stars are probably rare. The shape of the distribution implies that the scanning bias may be slight.

Of the 7 hyperfragments (H.F.), four have sufficient range (>10 μ) to be clearly separated from the K^- star; the others have ranges less than 2 μ. Six are nonmesonic decays, but one of the very short hyperfragments is a possible mesonic decay. All of the hyperfragments observed are produced in stars with eight or more prongs, and of the four largest stars (12 to 15 prongs), three give rise to hyperfragments.

The energy distribution of the charged Σ hyperons is shown in Fig. 1. A total of 25 prongs were identified as Σ particles by their subsequent decay in flight or by their interaction, either in flight or at rest. There was no clear case of a decay at rest. We have not as yet followed the secondaries from the Σ decays in flight, and thus no reliable estimate of the Σ^+/Σ^- ratio can be given. No estimates have been made of the number of Σ hyperons missed among 0-prong Σ^- interactions at rest nor among Σ^+ decays in flight via $\Sigma^+ \rightarrow p + \pi^0$, which may have been interpreted as small-angle proton scattering events.

Combining the numbers of hyperfragments and charged Σ hyperons, we find that about one-third of the stars yield visible negative strangeness.

We have observed seven interactions that lead to double-pion emission. In this sample of stars, no event was found in which both pions came to rest. However, one of the pair came to rest in six cases, and in all cases the accompanying pions were clearly identified by differential grain counting. A charged Σ hyperon was also produced in two examples exhibiting double-pion emission.

There were 35 events in which a single charged pion was emitted; of these, 13 were accompanied by a charged hyperon.

A total of 19 π^- and 9 π^+ mesons emitted from stars came to rest in the emulsion. Figure 2 presents the energy distribution of all the emitted pions. The general form of the distribution is a broad peak of the energies between 10 and 70 Mev, with a high-energy tail extending to about 700 Mev. The low-energy portion of the distribution can be attributed to the effects of multiple collisions of the pions within the nucleus before emission and to the general reduction of energy due to multiple pion production.

Three cases of K^- re-emission were observed. In each instance the kinetic energy was greater than 250 Mev, and none of these K mesons came to rest. The high energy of the K particles, together with the fact that there was no evidence for associated production, makes it unlikely that any of these particles were K^+ mesons.

(B) Analysis of selected events.– From those events selected according to criteria for Group (B) as described above, we have chosen 52 events which actually produced evidence of strange-particle production for this section. None of the events which comprise Group (A) are included in this analysis. The reasons for employing these criteria for the selection of events were to search more effectively for cascade particles, or evidence for them, and to place upon a firmer basis the reactions (a) and (b) that were observed or indicated in Group (A).

The results of these analyses are summarized in Table II.

Double-pion production [reaction (1)] was observed in 7 stars. In three of these, both pions were brought to rest. Two negative pions stopped in two of these cases ($\Sigma^+ + 2\pi^-$), and pions of op-

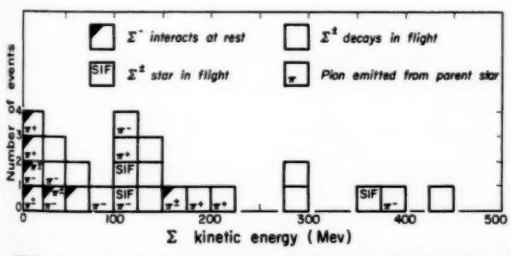

FIG. 1. Observed energy distribution of the charged Σ hyperons based upon an unbiased sample of 102 interactions.

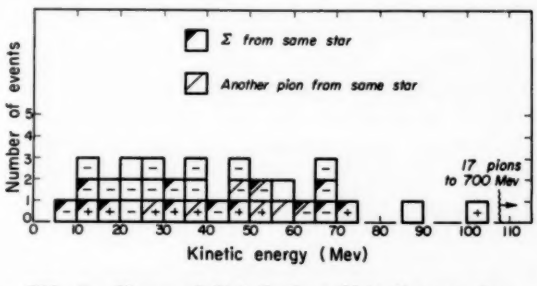

FIG. 2. Observed distribution of kinetic energies for the emitted charged pions. Charge is assigned for pions that came to rest in emulsion.

Table II. Summary of data on selected stars from which strange particles emerge.

Type	H.F., 0π	H.F., 1π	H.F., 2π	Σ, 0π	Σ, 1π	Σ, 2π	K^-, 0π	K^-, 1π	K^-, 2π	2Σ	2H.F.	Cascade H.F.
Number	11	6	0	11	7	6	1	3	1	4	1	1
Average stable prongs	6.4	6.9	...	4.9	3.3	3.2	4	2.0	2	3.75	3	6

posite charge stopped in the other ($\Sigma^- + \pi^- + \pi^+$). The pions were associated with Σ hyperons ($3\Sigma^+$, $2\Sigma^-$, $1\Sigma^\pm$) in six events and with a re-emitted K^- in one event. No event in which three or more charged pions were emitted was detected.

Five events were found that indicated production of two hyperons. Only one case was definite. In this case two prongs were hyperfragments, one undergoing mesonic decay and the other forming a two-prong star. In the less-well-defined events, all of the interactions emitted one Σ hyperon that was identified by its decay. In each instance, however, an additional prong interacted, either in flight or at rest, in such a manner as to indicate strongly that it was a Σ particle.

Only one K^- interaction displayed the necessary features for the emission of a cascade hyperfragment. (The absorption of a cascade particle in a nucleus is expected to yield two lambda hyperons of relatively low energy.) The event appears as a triple-centered star. The prongs are but several microns long and their identification was not possible. Although this event fits the criteria for a cascade hyperfragment as described above, an equally valid interpretation would be the formation of a hyperfragment by a slow Σ^- hyperon.

Inelastically scattered K^- mesons accompanied by 0, 1, and 2 pions were seen. The K^- particles were identified by their characteristic interactions (4 at rest, 1 in flight). The energy distribution of the re-emitted K^- mesons varied from 6 to 270 Mev. Despite the bias of our selection criteria, it appears significant that pions are so frequently produced in association with inelastic scattering. It also accounts for the broad energy spectrum of the scattered K^- mesons, which otherwise could be understood only by assumption of multiple collisions within the nucleus.

We wish to acknowledge the assistance afforded us during the emulsion exposure by Dr. Myron Good and Professor Harold K. Ticho. Our group of scanning technicians must be given recognition for their rapid and highly efficient work that contributed much to this study.

*This work was done under the auspices of the U. S. Atomic Energy Commission.

[1]Alvarez, Eberhard, Good, Graziano, Ticho, and Wojcicki, Phys. Rev. Lett. 2, 215 (1959).

Λ^0 AND Σ^0 PRODUCTION FROM THE (Σ^-, d) SYSTEM*

T. B. Day, G. A. Snow, and J. Sucher
Department of Physics, University of Maryland, College Park, Maryland
(Received May 14, 1959)

Recently a measurement has been reported on the Λ^0, Σ^0 branching ratio from the absorption of Σ^- hyperons in deuterium.[1] The result, based on 51 events, is

$$w_{\Sigma^0}(D)/[w_{\Sigma^0}(D) + w_{\Lambda^0}(D)] = 0.14 \pm 0.06, \quad (1)$$

where $w_Y(D)$ is the transition probability for the reaction

$$\Sigma^- + d \rightarrow Y + n + n. \quad (2)$$

The corresponding result for Σ^- absorption in hydrogen is[2]

$$w_{\Sigma^0}(H)/[w_{\Sigma^0}(H) + w_{\Lambda^0}(H)] = 0.33 \pm 0.05. \quad (3)$$

The purpose of this note is to inquire whether the results given in Eqs. (1) and (3) can be qualitatively understood within the framework of the simple impulse approximation. In this approximation the Σ^- is pictured as interacting only with the proton, and the effect of the neutron's

presence is ignored. In the (K^-, d) reaction,[3] the neutron has been shown[4] to enhance the Λ^0 mode via the two-step process

$$K^- + d \rightarrow \Sigma^+ + n + \pi^- \rightarrow \Lambda^0 + p + \pi^-. \quad (4)$$

The question might be raised as to whether a similar two-step process may be involved in accounting for the lower ratio of Eq. (1) as compared to Eq. (3).

We would like to point out that the result given in Eq. (1) does not constitute evidence for the enhancement of Λ^0 production relative to Σ^0 in deuterium. In fact, as will be seen below, the simplest assumptions imply just the reverse conclusion, namely, an enhancement of Σ^0 production.

We assume, for simplicity, that (*i*) the reaction of Eq. (2) takes place from the 1*S* orbit of the (Σ^-, d) system, (*ii*) the parity of both Σ^0 and Λ^0 relative to Σ^- is even, and (*iii*) final-state interactions can be neglected so that the final two-neutron wave function can be taken to be an antisymmetrized plane wave.

The most general *s*-wave interaction transition operator for the Σ^- reaction in hydrogen may then be written, for Σ^0 production,

$$t = a_0 1_{\Sigma^0,\Sigma^-} 1_{n,p} + a_1 \vec{\sigma}_{\Sigma^0,\Sigma^-} \cdot \vec{\sigma}_{n,p}. \quad (5)$$

For Λ^0 production, the constants a_0, a_1 are replaced by constants b_0 and b_1. The subscripts in Eq. (5) denote the particle spin-wave functions between which the unit operator, 1, or spin operator, $\vec{\sigma}$, acts.

Using Eq. (5), we find[5]

$$w_{\Sigma^0}(\mathrm{D})/w_{\Sigma^0}(\mathrm{H}) = J_{\Sigma^0} - \xi_{\Sigma^0} J_{\Sigma^0}', \quad (6)$$

and

$$w_{\Lambda^0}(\mathrm{D})/w_{\Lambda^0}(\mathrm{H}) = J_{\Lambda^0} - \xi_{\Lambda^0} J_{\Lambda^0}', \quad (7)$$

where

$$\xi_{\Sigma^0} = (|a_0|^2 + |a_1|^2)/(|a_0|^2 + 3|a_1|^2), \quad (8)$$

and ξ_{Λ^0} is similarly defined in terms of b_0 and b_1. The quantities J_Y and J_Y' are obtained by numerical integration. We find

$$J_{\Lambda^0} = 3.14, \quad J_{\Lambda^0}' = 0.976. \quad (9)$$

J_{Σ^0} and J_{Σ^0}' are quite sensitive to the Q value of the reaction of Eq. (2), and hence to the mass difference, $\Delta M = M_{\Sigma^-} - M_{\Sigma^0}$. Therefore we have evaluated these integrals for two choices of ΔM, and get

$$J_{\Sigma^0} = 0.585, \quad J_{\Sigma^0}' = 0.534, \quad (\Delta M = 6.0 \text{ Mev}),[6] \quad (10)$$

and

$$J_{\Sigma^0} = 0.164, \quad J_{\Sigma^0}' = 0.161, \quad (\Delta M = 4.45 \text{ Mev}).[2] \quad (11)$$

Values of the ratios in Eqs. (6) and (7) are listed in Table I for some simple choices of the parameters a_0, a_1, b_0, b_1. In this table, the first

Table I. Deuterium to hydrogen hyperon-production ratios.

$a_0 : a_1$	$w_{\Sigma^0}(\mathrm{D})/w_{\Sigma^0}(\mathrm{H})$ $\Delta m^a = 6.0$	$\Delta m = 4.45$	$b_0 : b_1$	$w_{\Lambda^0}(\mathrm{D})/w_{\Lambda^0}(\mathrm{H})$
1 : 0	0.051	0.003	1 : 0	2.16
0 : 1	0.407	0.110	0 : 1	2.82
$\frac{1}{2} : \frac{1}{2}$	0.318	0.084	$\frac{1}{2} : \frac{1}{2}$	2.65
$\frac{3}{2} : -\frac{1}{2}$	0.140	0.030	$\frac{3}{2} : -\frac{1}{2}$	2.33

[a] $\Delta m = m_{\Sigma^-} - m_{\Sigma^0}$ in Mev.

and second lines correspond to minimum and maximum values, respectively, for these ratios. The third and fourth lines correspond, respectively, to

$$t \sim 1_{\Sigma^0,p} 1_{n,\Sigma^-}, \quad (12)$$

and

$$t \sim \vec{\sigma}_{\Sigma^0,p} \cdot \vec{\sigma}_{n,\Sigma^-}, \quad (13)$$

as a consequence of the identities

$$1_{\Sigma^0,p} 1_{\Sigma^-,n} = \tfrac{1}{2} 1_{\Sigma^0,\Sigma^-} 1_{n,p} + \tfrac{1}{2} \vec{\sigma}_{\Sigma^0,\Sigma^-} \cdot \vec{\sigma}_{n,p}, \quad (14)$$

and

$$\vec{\sigma}_{\Sigma^0,p} \cdot \vec{\sigma}_{\Sigma^-,n} = \tfrac{3}{2} 1_{\Sigma^0,\Sigma^-} 1_{n,p} - \tfrac{1}{2} \vec{\sigma}_{\Sigma^0,\Sigma^-} \cdot \vec{\sigma}_{n,p}. \quad (15)$$

In order to compare with experiment, we compute

$$w_{\Lambda^0}(\mathrm{D})/w_{\Sigma^0}(\mathrm{D}) = [w_{\Lambda^0}(\mathrm{D})/w_{\Lambda^0}(\mathrm{H})] \times [w_{\Sigma^0}(\mathrm{D})/w_{\Sigma^0}(\mathrm{H})]^{-1} [w_{\Lambda^0}(\mathrm{H})/w_{\Sigma^0}(\mathrm{H})], \quad (16)$$

where $w_{\Lambda^0}(\mathrm{H})/w_{\Sigma^0}(\mathrm{H})$ is obtained from the experimental value given in Eq. (3). Table II lists the ratio $w_{\Lambda^0}(\mathrm{D})/w_{\Sigma^0}(\mathrm{D})$ for three choices of the parameters.

The value 10.8 for $w_{\Lambda^0}(\mathrm{D})/w_{\Sigma^0}(\mathrm{D})$, given in

Table II. Λ^0 to Σ^0 production ratios in deuterium.

$(a_0:a_1)$	$(b_0:b_1)$	$w_{\Lambda^0}(D)/w_{\Sigma^0}(D)$ $\Delta m=6.0$	$\Delta m=4.45$
1:0	1:0	86.0	1460
0:1	0:1	14.1	52.0
0:1	1:0	10.8	39.9
Experiment			$6.2^{+5.3}_{-2.2}$

Table II, is the absolute minimum value for this ratio with the basic assumption of s-wave interaction, and the assumptions (*i*)-(*iii*) listed above. It is clear from Table II that if the (Σ^-,Σ^0) mass difference is as small as 4.45 Mev, it is impossible to obtain a value for $w_{\Lambda^0}(D)/w_{\Sigma^0}(D)$ within the experimental range. It may also be seen that for either value of ΔM, the smallest (Λ^0/Σ^0) ratios are obtained when the Σ^0 production transition operator is of the form $\vec{\sigma}_{\Sigma^0}, \Sigma^- \cdot \vec{\sigma} n,p$. Since the minimum theoretical value of the (Λ^0/Σ^0) ratio is still high compared to the experimental result, there is no need to invoke an appreciable amount of a two-step process which would enhance the Λ^0 production in deuterium.

There are two important ways in which the above results may be modified. One modification will arise from including the effect of final-state interactions in the (Σ^0,nn) system.[8,9] The other modification would be present if, as may very well be the case, an appreciable number of Σ^- captures in hydrogen were to take place from P orbits. In that case, there would no longer be a simple connection between the Σ^- capture events in hydrogen and deuterium.

We would like to thank Dr. G. Feinberg for a useful conversation.

*This research was supported in part by the U. S. Atomic Energy Commission and by the U. S. Air Force through the Air Force Office of Scientific Research of the Air Research and Development Command.

[1]Horwitz, Miller, and Murray, Bull. Am. Phys. Soc. Ser. II, 4, 298 (1959).

[2]A. H. Rosenfeld, Bull. Am. Phys. Soc. Ser. II, 3, 363 (1959).

[3]Horwitz, Miller, Murray, Schwartz, and Taft, Bull. Am. Phys. Soc. Ser. II, 3, 377 (1958).

[4]R. Karplus and L. Rodberg, Bull. Am. Phys. Soc. Ser. II, 4, 38 (1959).

[5]The method of calculation is exactly similar to the one in reference 7 for the reaction $K^- + d \to \bar{K}^0 + 2n$, except that the capture from a bound state simplifies the integrations. (In particular, the β-dependent terms which arise from the Hulthén wave-function for the deuteron, are neglected, since $\beta \sim 6.2\alpha$.) Similar calculations have been done for $\pi^- + d$ reactions. See, e.g., Fernbach, Green, and Watson, Phys. Rev. 84, 1084 (1951).

[6]M. L. Stevenson, Phys. Rev. 111, 1707 (1958).

[7]Day, Snow, and Sucher, Nuovo cimento (to be published).

[8]The final-state interaction in the (Λ^0,nn) system is expected to be small, since a closure calculation[7] of $w_{\Lambda^0}(D)/w_{\Lambda^0}(H)$ gives 3.02 for the choice $b_0:b_1=1:0$. However, since the energy available to the (Σ^0,nn) system is so much smaller, the transition probability in this case should be much more sensitive to final-state interactions. In face, a closure calculation in the case $\Delta m=4.45$ Mev and $a_0:a_1=0:1$ gives $w_{\Sigma^0}(D)/w_{\Sigma^0}(H)=1.33$. Using this value in Eq. (16) gives $w_{\Lambda^0}(D)/w_{\Sigma^0}(D)=3.24$. This result, while presumably a gross underestimate, indicates the probable importance of final-state interaction.

[9]If one assumes that the Σ^0 and Σ^- have opposite parities, a crude estimate for the case $\Delta m=6.0$ Mev indicates that the minimum ratio of Λ^0 to Σ^0 production in deuterium will not be altered appreciably.

MEASUREMENT OF THE π^0 MASS, AND SEARCH FOR A π_0^0*

M. Gettner, L. Holloway, D. Kraus, K. Lande, E. Leboy, and W. Selove
Department of Physics, University of Pennsylvania, Philadelphia, Pennsylvania

and

R. Siegel
Department of Physics, Carnegie Institute of Technology, Pittsburgh, Pennsylvania
(Received April 29, 1959)

Although the mass of the π^0 meson has been reported[1] measured with an accuracy of about $0.3m_e$ (electron masses), the experiments on which this result is based were analyzed on the assumption that only a single π^0 exists, and these experiments could in fact have failed to detect the existence of two different π^0 mesons if two were produced in the reaction studied,

$$\pi^- + p \rightarrow n + \pi^0 \searrow 2\gamma. \qquad (1)$$

Since the "existence" of a second neutral meson π_0^0, with isotopic spin $T=0$, may be expected in addition to the ordinary π^0 meson ($T=1$), and since the possibility that the masses of π_0^0 and π^0 might be relatively close does not appear excluded by present knowledge,[2] it appears worthwhile to carry out a more direct measurement to determine the mass or masses. We report here the results of a preliminary experiment for this purpose. This work gives the first direct demonstration, to our knowledge, of a neutron group corresponding to a well-defined π^0 mass. Accompanying this result is a direct measurement of a lower limit on the lifetime of this meson.

π^- mesons were stopped in a thin (2 cm) liquid hydrogen target, and the neutrons produced were measured by time of flight, with an arrangement indicated in Fig. 1. A "zero-time" signal from the γ-detector was demanded for each neutron-detector signal recorded; the γ-detector signal was further required to be in close time coincidence (within about 10 nanoseconds $= 10\times10^{-9}$ sec), with an incoming particle in the π^- beam.

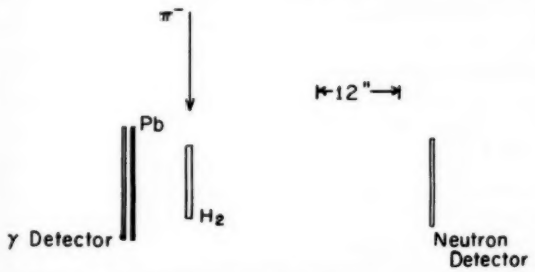

FIG. 1. Experimental arrangements.

Peaks in the time-of-flight distribution were observed corresponding to the two types of reaction khown to occur for π^- mesons stopped in hydrogen, namely reaction (1) above and

$$\pi^- + p \rightarrow n + \gamma. \qquad (2)$$

Another group was observed near zero flight time. Such a group is expected for $\pi^0 \rightarrow 2\gamma$ events in which the "neutron" detector responds to one of the γ rays. The "zero-flight-time" group also includes some background events, coming from neutron stars produced by π^- capture in the hydrogen target structure.

The time-of-flight distribution for a neutron detector distance of 3 feet is shown in Fig. 2. The zero of the abscissa scale is determined by electronic time delays in various legs of the recording system. The group at $\Delta t = 59$ is the "zero-flight-time" group, and that at $\Delta t = 78$ is the 8.8-Mev group from reaction (2) above. The intrinsic time resolution of the system, measured separately, was about 2 nanoseconds (full width at half-maximum). The position of γ-γ events (and consequently the position of true zero time of flight) in the group at $\Delta t = 59$ can be narrowed down by making use of pulse-height information from the neutron detector. From the data of Fig. 2, the energy of the 8.8-Mev group is found to agree with the value calculated from the known masses of π^-, neutron, and proton, to an accuracy corresponding to about 1 nanosecond of flight time.

A group of neutrons of approximately 0.4 Mev energy is expected from reaction (1). As calculated from the previously reported calculated best value for the mass difference[1]

$$m_{\pi^-} - m_{\pi^0} = (9.0 \pm 0.3)m_e, \qquad (3)$$

this group should occur at approximately the position of the arrow in Fig. 2. No group near this position showed clearly in these data. It

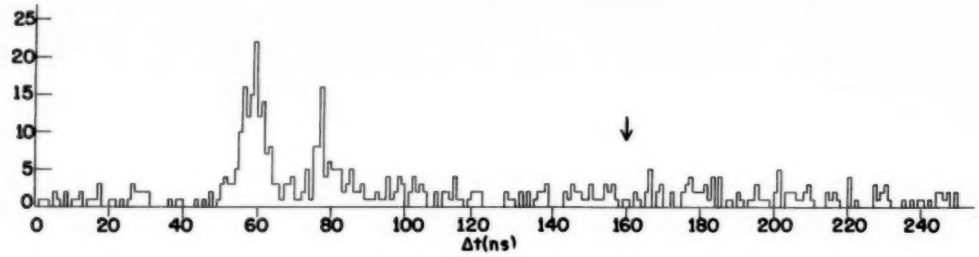

FIG. 2. Time-of-flight distribution for a neutron detector flight path of 3 feet. Number of events per 1-nanosecond (ns) interval is plotted against time difference between γ-detector and neutron-detector signals. Neutron-detector signals of all sizes are included.

could be expected that the effective background intensity contributing in Fig. 2 could be reduced by accepting only those neutron-detector pulses meeting an appropriate pulse-height requirement, but even so no clear group could be identified in the data.

Further data were taken with a shorter flight path, two feet, to reduce background. The result of this run, in the vicinity of the expected group, and with an appropriate choice as to maximum acceptable pulse height for the neutron-detector signal, are shown in Fig. 3(a). Here a group shows clearly, at about 32 nanoseconds/foot, near the expected position.

The 2-foot data of Fig. 3(a) and the 3-foot data of Fig. 2, combined (using the same value for the maximum acceptable pulse height), give the results in Fig. 3(b). The principal peak corresponds to a mass difference

$$m_{\pi^-} - m_{\pi^0} = (9.6 \pm 0.5) m_e. \quad (4)$$

The uncertainty given is due principally to (estimated) uncertainty in the exact position of true zero on the time-of-flight scale.

The result (4) is consistent with the previous best value (3). The existence of a π^0 meson with approximately the mass previously assigned to it is thus directly verified.

Although the existence of a second neutral π meson, the π_0^0, with mass near that of the π^0, cannot be strongly expected on the basis of previous knowledge, the data of Fig. 3 do not exclude the existence of such a π_0^0 with high confidence. The bump in the vicinity of 40 nanoseconds/foot, although of obviously poor statistical significance,

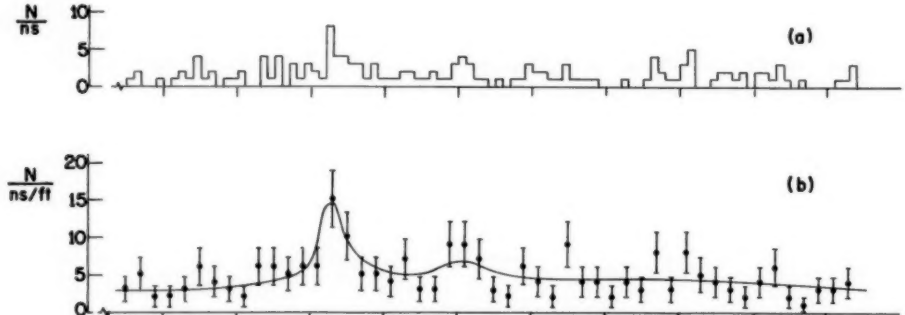

FIG. 3. (a) Data for neutron detector flight path of 2 feet. The abscissas give time difference (per foot) with respect to γ-γ signals. A neutron-detector-signal maximum pulse-height limit was imposed corresponding to neutrons of about 0.5-Mev energy. (b) Distribution consisting of (a) added to those events from the data of Fig. 2 satisfying the pulse-height criterion used in (a).

nevertheless consists principally of a group of events having neutron-detector pulse height appropriate to a neutron group of this time-of-flight. (The corresponding mass of the "second π^0" would be about 1.3 Mev heavier than that corresponding to the group at 32 nanoseconds/foot.) More refined measurements, which we hope to carry out, will be necessary to permit a more positive statement concerning a possible second group.

With more refined measurements it should also be possible to obtain a check of the Panofsky ratio.

Finally, the present results give directly a lower limit on the lifetime of the π^0 meson. This value is obtained through the uncertainty principle $\Gamma\tau \approx \hbar$, where Γ is the energy width of the π^0 and τ is the mean life. The degree of sharpness of the π^0 mass shown by the data gives

$$\tau > 3\times10^{-21} \text{ sec.} \qquad (5)$$

This value is far below the value expected theoretically.[3] It may be of some interest, however, since it is the first direct measurement giving a lower limit on the lifetime of the π^0 meson. Other experimental information on the lifetime is discussed, with references, in the report of Harris et al.,[4] which also gives an upper limit to the lifetime. It is true, however, that other measurements exist which, although less direct than the present one, have been analyzed to give a lower limit of 10^{-19} sec for the mean life.[5,6] It may be remarked that extending the present approach to the limit that at this time appears practical could be expected to cover the lifetime range up to 10^{-19}–10^{-18} sec.

We are extremely grateful to Dr. R. B. Sutton and to the staff of the Carnegie Institute of Technology synchrocyclotron for making the facilities of the laboratory available to us and for their generous assistance in this work.

---

*Supported by the U. S. Atomic Energy Commission.

[1] Cohen, Crowe, and Dumond, Fundamental Constants of Physics (Interscience Publishers, New York, 1957), p. 47.

[2] W. Selove (to be published).

[3] See M. L. Goldberger and S. B. Treiman, Nuovo cimento 9, 461 (1958).

[4] Harris, Orear, and Taylor, Phys. Rev. 106, 327 (1957).

[5] L. Osborne (private communication).

[6] F. E. Low (private communication).

POLARIZATION OF RECOIL PROTONS FROM THE PHOTOPRODUCTION OF π^0 MESONS FROM HYDROGEN*

P. C. Stein
Cornell University, Ithaca, New York
(Received May 4, 1959)

Sakurai[1] has pointed out that Peierls'[2] assignment of $D_{3/2}$ for the second resonance in photopion production predicts a strong polarization of the recoil protons from the reaction $\gamma + p \rightarrow p + \pi^0$ in the region of the second resonance. In particular, it can be shown that if an appreciable polarization is found at a recoil proton angle of 90° in the center-of-mass system at photon energies in the region of about 600 Mev, the parity of the 700-Mev resonances must be opposite to the parity of the 300-Mev resonance.

The polarization of the proton recoils has been measured at photon energies of 550 Mev and 700 Mev at a center-of-mass angle of 90° by allowing the protons to be incident upon a carbon scatterer and observing the left-right asymmetry in the scattering. The apparatus is shown in Fig. 1. The photon beam from the Cornell electron synchrotron is incident upon a vacuum liquid-hydro-

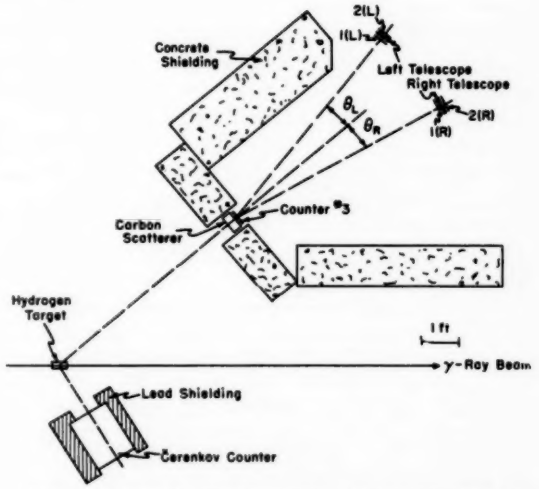

FIG. 1. Experimental apparatus for measuring the recoil proton polarization in the reaction $\gamma + p \rightarrow p + \pi^0$.

gen target. Protons at 40.5° in the laboratory are incident upon a carbon scatterer, and scatterings at 11.5° in the laboratory both to the left and right are measured. A totally absorbing lead glass Čerenkov counter is used to detect one of the decay photons from the π^0. All of the proton counters are plastic scintillation counters 4 in. wide by 16 in. long by 1 in. thick. The left and right telescopes each consist of two counters with brass absorbers between them. The two counters are run in coincidence, so that the absorber determines the minimum energy of a scattered proton that can be counted. The maximum energy of the detected proton is determined by the peak of the bremsstrahlung spectrum, which is kept at 150 Mev above the photon energy corresponding to the minimum energy proton that will count. The carbon scatterer subtends an angle of $\pm 2°$, and the Čerenkov counter an angle of $\pm 15°$ in the horizontal plane. The large angle subtended by the Čerenkov counter reduces the effect of a nonuniform irradiation of the carbon scatterer due to an energy-dependent change in the decay kinematics of the π^0. Scattered recoil protons were identified as events of the type $[1(L)+2(L)+3+C]$ and $[1(R)+2(R)+3+C]$. Events of the type $[1(L)+2(L)+3]$ and $[1(R)+2(R)+3]$, which consisted mostly of scattered mesons, were also recorded.

Biases on all the counters were set by alternately moving the left and right telescopes in line with the carbon scatterer and the hydrogen target, and thus counting unscattered protons. With the telescopes in the "in line" position, various kinematic checks were made to ensure that the coincidences counted were due to the reaction $\gamma+p\rightarrow p+\pi^0$. During the course of the experiment, the left and right telescopes were interchanged repeatedly. No statistically significant difference was found between the responses of these two telescopes.

Both telescopes as well as the carbon scatterer were rigidly mounted on an aluminum frame, and the frame was lined up with the hydrogen target optically. The difference between the left and right scattering angle was less than 0.1°.

Runs taken with an empty hydrogen target gave intensities of a few percent of the ratio with a full target.

The pulse height of each scattered proton in the first counter in the telescope was recorded, and the distributions agreed with the pulse-height spectra taken with the telescope in the "in line" position.

The polarization of the recoil protons was calculated from the experimental data by means of a Monte Carlo calculation. The data of Haffner[3] on the polarization of elastically scattered protons from carbon at 220 Mev were used for the analysis of the 700-Mev point, and those of Alphonse[4] at 155 Mev for the 550-Mev point. In order to interpolate to energies near those measured points, it was assumed that the polarization in scattering was a function only of the momentum transfer. The effects of inelastic scattering were calculated from the cross sections of Tyrén and Maris[5] and the polarization data of Bradner and Donaldson.[6] The Monte Carlo calculation was performed both including and neglecting the effect of inelastic scattering. The calculated polarization of the recoil proton from π^0 production differed in the two cases by 0.04. The calculation was performed twice. In one case, a proton polarization of -1.00 was assumed and in the other, a polarization of zero was assumed. The results of both calculations, in terms of the relative probabilities for a left and right scattering, are shown in Table I. Since these relative probabilities are a linear function of the polarization of the incoming protons, we are able to compute the polarization from the experimental asymmetry.

At the 550-Mev point, 116 left counts and 90 right counts were observed; at the 700-Mev point, 530 left counts and 280 right counts were observed.

Since mesons, having a spin of 0, cannot have any left-right scattering asymmetry, a compari-

Table I. Results of the Monte Carlo calculation. The last column shows the value of the polarization calculated from the experimental asymmetry.

	Relative probability for a left count $P=-1$ (arbitrary units)	Relative probability for a right count $P=-1$ (arbitrary units)	Relative probability for a left count $P=0$ (arbitrary units)	Relative probability for a right count $P=0$ (arbitrary units)	Polarization of recoil protons from $\gamma+p\rightarrow p+\pi^0$
700 Mev	84	382	217	238	0.59 ± 0.06
550 Mev	76	281	166	181	0.30 ± 0.12

son of the two coincidence rates without the Čerenkov counter requirement serves as a check of the equipment. After correcting for the background rates and subtracting out the true proton coincidences, there was no statistically significant difference in the $[1(L)+2(L)+3]$ and $[1(R)+2(R)+3]$ rates.

In Table I are shown the values of the polarization of the recoil protons from π^0 production computed from the experimental data as well as the results of the Monte Carlo calculations. The sign of the polarization is in the direction of $\vec{K}_0 \times \vec{K}_p$, where $\vec{K}_0$ is the photon momentum and $\vec{K}_p$ the recoil proton momentum.

Additional evidence for the polarization at the 550-Mev point is provided by a nuclear emulsion experiment.[7] Preliminary results give a most likely value of $P = +0.3$.

The large value of the polarization at 700 Mev indicates strongly that the parity of the second resonance is opposite to the parity of the 300-Mev resonance, i.e., negative. The sign of the polarization is as predicted.[8] The fact that the polarization is greater at 700 Mev indicates that the contributions of the two resonances are more nearly equal at this energy than at 550 Mev.

---

*Supported in part by the joint program of the Office of Naval Research and the U.S. Atomic Energy Commission.

[1]J. J. Sakurai, Phys. Rev. Lett. 1, 258 (1958).
[2]R. F. Peierls, Phys. Rev. Lett. 1, 174 (1958).
[3]E. M. Haffner, Phys. Rev. 111, 297 (1958).
[4]Alphonse, Johansson, and Tibell, Nuclear Phys. 3, 185 (1957).
[5]H. Tyrén and T. A. J. Maris, Nuclear Phys. 3, 52 (1957).
[6]H. Bradner and R. Donaldson, Phys. Rev. 95, 1701 (1954).
[7]P. L. Connolly and R. Weill, Bull. Am. Phys. Soc. Ser. II, 4, 23 (1959), and private communication.
[8]R. F. Peierls (private communication).

MANY-CHANNEL UNITARITY CONDITION*

Richard H. Capps
Laboratory of Nuclear Studies, Cornell University, Ithaca, New York
(Received May 4, 1959)

Many useful relations concerning particle reaction problems are known to follow from the unitarity of the reaction matrix. For example, Watson has shown that if there are only two channels open, the requirements of unitarity and time-reversal invariance imply that the phase of the inelastic amplitude is equal to the sum of the phase shifts for the two elastic processes.[1] It is the purpose of this note to derive a useful generalization of this theorem to the case when many channels are open, and to illustrate the generalization by applying it to photoproduction of mesons at 600 Mev.

We consider the reaction matrix in the center-of-mass system for a set of states of arbitrary numbers of particles, the states being connected by strong and electromagnetic interactions. We imagine the system to be enclosed in a large volume so that all quantum numbers are discrete; this assumption is made only for convenience and does not affect the final results. A representation is chosen in which the total angular momentum, z component of angular momentum, and parity are diagonal. The reaction matrix T is defined in terms of the unitary S matrix by the equation $iT = S - 1$, where 1 is the unit matrix. The diagonal elements of S are denoted by $S_{\alpha\alpha} = (1 - R_\alpha)\exp(2i\delta_\alpha)$, where δ_α is the real phase shift, and R_α, the real absorption coefficient, satisfies the inequality $0 \leq R_\alpha \leq 1$.

We now define a new matrix V by the equation, $iV_{\alpha\beta} = S_{\alpha\beta}\exp[-i(\delta_\alpha + \delta_\beta)]$. The requirement of time-reversal invariance implies that, with a suitable choice of phase relations between the states, the S matrix is symmetric,[2] i.e., $S_{\alpha\beta} = S_{\beta\alpha}$. It is easy to see that the symmetry and unitarity of S imply the symmetry and unitarity of V. The matrix V is simpler than S in that the diagonal elements of iV are real. If one equates the absolute square of both sides of the unitarity equation

$$\sum_{\beta=1}^{2} V_{1\beta} V_{2\beta}^{*} = -\sum_{\beta>2} V_{1\beta} V_{2\beta}^{*},$$

and makes use of the relations, $V_{\alpha\beta} = V_{\beta\alpha}$ and $iV_{\alpha\alpha} = (1 - R_\alpha)^{1/2}$, the result may be written in the form

$$\cos(2\theta_{12}) = \frac{1-\frac{1}{2}(R_1+R_2)-\frac{1}{2}(|\sum_{\beta>2} V_{1\beta}V_{2\beta}^*|^2/|V_{12}|^2)}{(1-R_1)^{1/2}(1-R_2)^{1/2}}, \quad (1)$$

where θ_{12} is the phase of V_{12}, i.e., $V_{12} = |V_{12}| \times \exp(i\theta_{12})$.

If only two channels are open, the sum over β vanishes, and it is further required by unitarity that $R_1 = R_2$. In this case Eq. (1) reduces to the form $\cos(2\theta_{12}) = 1$. Since $T_{12} = V_{12}\exp[i(\delta_1+\delta_2)]$, this is the familiar theorem[1] that the phase of the inelastic amplitude T_{12} is either $(\delta_1+\delta_2)$ or $(\delta_1+\delta_2+\pi)$.

The phase of any one inelastic amplitude is, of course, not measurable. However, the results of angular distribution and polarization measurements depend upon the relative phases of the amplitudes for different angular momentum and parity states of a given set of final particles. The requirement of a symmetric T matrix implies a definite choice of phase relations between angular momentum states.[3] Hence the unitarity condition allows one to relate angular distribution and polarization measurements of inelastic processes to similar measurements of elastic processes.

In order to interpret Eq. (1), it is useful to relate the quantities in the equation to cross sections. If α represents a two-particle state, we use the symbol $\sigma_\alpha^{\max}$ to denote the maximum inelastic cross section consistent with unitarity for unpolarized particles in the initial state α. Thus $\sigma_\alpha^{\max} = \pi(2j+1)(N_a N_b)^{-1}(\hbar/p_i)^2$, where p_i is the initial particle momentum, j is the total angular momentum quantum number, and N_a and N_b are the numbers of spin states of the two particles in the state α. It follows from the unitarity of S that (for $\alpha \neq \beta$), $|V_{\alpha\beta}|^2 = |T_{\alpha\beta}|^2 = \sigma_{\alpha\beta}/\sigma_\alpha^{\max}$ and $R_\alpha = \sum_{\gamma\neq\alpha}|V_{\alpha\gamma}|^2 = \sigma_\alpha^{\text{in}}/\sigma_\alpha^{\max}$, where $\sigma_{\alpha\beta}$ is the actual (unpolarized) cross section from state α to state β, and $\sigma_\alpha^{\text{in}}$ is the corresponding total inelastic cross section from the initial state α.

We illustrate the applicability of Eq. (1) to a case in which more than two channels are open by considering the relation of photoproduction of pions from protons to pion-nucleon scattering at energies where two meson states are important. Peierls[4] and Sakurai[5] have discussed the angular distribution and polarization in the process $\gamma+p\to p+\pi^0$ on the basis of a model in which the two dominant processes are production of even- and odd-parity $j=\frac{3}{2}$ pion-nucleon states by magnetic and electric dipole photons, respectively. The model has had considerable success in explaining and predicting experimental results.[6] It is assumed in this model that the photoproduction phases are related to pion-nucleon scattering phases. We may use Eq. (1) to show that such a phase relation can be established. We consider those states corresponding to $j=\frac{3}{2}$, even parity, and unit positive charge, and label the different channels with the following indices: (1) photon-proton magnetic dipole state; (2) pion-nucleon in total isotopic spin $\frac{3}{2}$ state; (3 and higher) all other states, including multiple meson states. The amplitude T_{12} is then proportional to the amplitude A of references 4 and 5, the proportionality constant being real. We now use Eq. (1) to place limits on θ_{12}. Isotopic spin conservation in pion-nucleon processes implies that $V_{2\beta}=0$ if β denotes a state involving a nucleon and one or more mesons corresponding to a total isotopic spin other than $\frac{3}{2}$. Hence such $I\neq\frac{3}{2}$ states may be excluded from the sum over β in Eq. (1). We define the quantities W_1 and W_2 by the relations

$$W_1 = \sum_{\beta>2}|V_{1\beta}|^2, \quad W_2 = \sum_{\beta>2}|V_{2\beta}|^2,$$

where $I\neq\frac{3}{2}$ states are excluded from the sums. Application of the Schwartz inequality to Eq. (1) leads to the result

$$(1-R_1)^{1/2}(1-R_2)^{1/2}\cos(2\theta_{12}) \geq 1-\tfrac{1}{2}(R_1+R_2) - \tfrac{1}{2}(W_2W_1/|V_{12}|^2). \quad (2)$$

The quantities R_1, R_2, W_2 and $W_1/|V_{12}|^2$ may be estimated from experimental data. We consider an energy corresponding to 600-Mev lab photon energy in channel 1, or 450-Mev lab pion kinetic energy in channel 2. Since R_1 is proportional to the square of the electric charge, it is small and may be neglected. The ratio $W_1/|V_{12}|^2$ is equal to the cross-section ratio σ_1'/σ_{12}, where σ_1' is the cross section for the production from channel 1 of two or more mesons in a state of total isotopic spin $\frac{3}{2}$ (if the weak radiative processes are neglected). The cross section σ_{12} has been estimated to be 55 microbarns at this energy.[4] In order to estimate σ_1' we observe that the total cross section for the process $\gamma+p\to\pi^+ +\pi^-+p$ is about 60 microbarns.[7] The cross sections for production of $(2\pi^0+p)$ and $(\pi^+ +\pi^0+n)$ states are not known, but may also be of this order. It is probable that most of the multiple meson production at this energy is related to the

pion-nucleon 600-Mev scattering resonance and hence occurs in the $I=\frac{1}{2}$ state. Since σ_1' represents only the partial cross section for magnetic dipole photons leading to $j=\frac{3}{2}$, $I=\frac{3}{2}$ states, it is certainly reasonable to assume that $\sigma_1'<100$ μb. Hence we assume $W_1/|V_{12}|^2<2$. In order to estimate R_2, we note that at 450 Mev lab energy the total inelastic cross section for an incident π^+-proton state ($I=\frac{3}{2}$ state) has been measured to be less than 2.5 millibarns.[8] Hence the partial cross section σ_2^{in} must also be less than 2.5 mb. Since the maximum possible partial inelastic cross section $\sigma_2^{\max}$ at this energy is 17.5 mb, it is seen that $R_2<0.15$. By definition W_2 satisfies the inequality $W_2<R_2$. We conclude that R_1, R_2, W_2, and $W_1/|V_{12}|^2$ satisfy the relations $R_1\approx 0$, $R_2<0.15$, $W_2<R_2$, and $W_1/|V_{12}|^2<2$. From these relations and Eq. (2) it can be shown that $\cos(2\theta_{12})>0.84$. Therefore, the phase ϕ_{12} of the amplitude T_{12} must satisfy one of the two inequalities,

$$|\phi_{12}-\delta_2|<17^\circ \quad \text{or} \quad |\phi_{12}-\delta_2-\pi|<17^\circ, \tag{3}$$

where the small photon scattering phase δ_1 has been neglected. Thus the phase relation characteristic of the two-channel case is nearly satisfied here, even though several channels are important.

The amplitudes for production of a p-π^0 state are linear combinations of the amplitudes for production of $I=\frac{1}{2}$ and $I=\frac{3}{2}$ pion-nucleon states. In the model of references 4 and 5 however, the $I=\frac{1}{2}$, $j=\frac{3}{2}$ magnetic dipole state is neglected, so that the phase ϕ_{12} of Eq. (3) above is equal to the phase of the $j=\frac{3}{2}$, magnetic dipole amplitude for the process $\gamma+p\to p+\pi^0$. Similar results may be obtained for the phases of other angular momentum and parity states. In this manner polarization and angular distribution measurements of photoproduction may be related to similar measurements of pion-nucleon scattering.

An interesting discussion concerning this subject was had with Ronald F. Peierls.

---

* Supported by the joint program of the Office of Naval Research and the U. S. Atomic Energy Commission.

[1] K. M. Watson, Phys. Rev. 95, 228 (1954); see also M. Gell-Mann and K. M. Watson, Annual Review of Nuclear Science (Annual Reviews, Inc., Stanford, 1954), Vol. 4, p. 219, Appendix.

[2] F. Coester, Phys. Rev. 89, 619, (1953).

[3] The choice is definite except that the phase of any state (and hence of all nondiagonal elements of T involving this state) may be increased by π without destroying the symmetry of T. See reference 2.

[4] Ronald F. Peierls, Phys. Rev. Lett. 1, 174 (1958).

[5] J. J. Sakurai, Phys. Rev. Lett. 1, 258 (1958).

[6] P. C. Stein (to be published). Other experimental references are listed in reference 4.

[7] Sellen, Cocconi, Cocconi, and Hart, Phys. Rev. 110, 779 (1958).

[8] Blevins, Block, and Leitner, Phys. Rev. 112, 1287 (1958).

RADIATIVE CORRECTIONS TO π-e DECAY*

Toichiro Kinoshita
Laboratory of Nuclear Studies, Cornell University, Ithaca, New York
(Received May 11, 1959)

As is well known, the ratio of probabilities for π-e and π-μ decays is given by[1]

$$R_0=\left(\frac{m_e}{m_\mu}\right)^2\left(\frac{m_\pi^2-m_e^2}{m_\pi^2-m_\mu^2}\right)^2=1.28\times10^{-4}, \tag{1}$$

neglecting electromagnetic corrections, if the decay interaction is assumed to be

$$ig\bar{\psi}_l\gamma_\mu a\psi_\nu(\partial\varphi_\pi/\partial x_\mu), \tag{2}$$

where $a=(1+i\gamma_5)/2$ and l represents either muon or electron. This interaction is consistent[2] with the hypothesis of universal V-A interaction of Fermi couplings.[3] Recent experiments[4] support these assumptions strongly. The new measurements are becoming sufficiently accurate to justify a calculation of the effect of radiative corrections. This problem has recently been studied by Berman,[5] who has found surprisingly large corrections to π-e decay. In this note it is attempted to understand the reason why the radiative corrections are so large. We are also interested to see whether the pion decay agrees with the recently conjectured "theorem"[6] that the radiative correction to the total probability of a decay process is finite in the limit where the

mass of the secondary electron is assumed to be arbitrarily small, although corrections to partial probabilities may be divergent in such a limit.

We first calculated the probability for the inner bremsstrahlung (IB) process in which the pion disintegrates into electron, neutrino, and photon.[7] We integrate it over all neutrino and photon momenta to find the energy spectrum of the electron.[8] Integrating it further over the electron energy, the probability of observing any electron whose energy is less that $E_{\max} - \Delta E$ is found to be

$$\frac{\Delta P_{\mathrm{IB}}(\Delta E)}{P_0} = \frac{\alpha}{\pi}\left\{-b(\mu)\left[\ln\left(\frac{m_\pi}{2\Delta E}\right) + 2\ln(1-\mu^2) - \tfrac{3}{4}\right] - \frac{\mu^2(10-7\mu^2)}{2(1-\mu^2)^2}\ln\mu + \frac{2(1+\mu^2)}{1-\mu^2}L(1-\mu^2) + \frac{15-21\mu^2}{8(1-\mu^2)}\right\}, \tag{3}$$

where P_0 is the uncorrected rate of decay,

$$L(x) = \int_0^x \ln(1-t)(dt/t), \quad \mu = m_e/m_\pi,$$

$$b(\mu) = 2\left(\frac{1+\mu^2}{1-\mu^2}\ln\mu + 1\right),$$

and ΔE is assumed to be small compared with the maximum energy $E_{\max} = m_\pi(1+\mu^2)/2$. The total probability of inner bremsstrahlung is given by

$$\frac{\Delta P_{\mathrm{IB}}}{P_0} = \frac{\alpha}{\pi}\left\{b(\mu)\left[\ln\left(\frac{\lambda_{\min}}{m_\pi}\right) - \ln(1-\mu^2) - \tfrac{1}{2}\ln\mu + \tfrac{3}{4}\right] - \frac{\mu^2(10-7\mu^2)}{2(1-\mu^2)^2}\ln\mu + \frac{2(1+\mu^2)}{1-\mu^2}L(1-\mu^2) + \frac{15-21\mu^2}{8(1-\mu^2)}\right\}. \tag{4}$$

This contains an infrared divergence since photons of very low energy (with infinitesimal mass $\lambda_{\min}$) are emitted near the maximum electron energy.

To find the correction due to virtual emission and reabsorption of photons, let us note that the interaction (2), or more precisely

$$g\bar{\psi}_l\gamma_\mu a\psi_\nu(i\partial\varphi_\pi/\partial x_\mu - eA_\mu\varphi_\pi), \tag{5}$$

is equivalent to

$$gm_l^0\bar{\psi}_l a\psi_\nu\varphi_\pi, \tag{6}$$

in the lowest order in g and to any order in e, where m_l^0 is the bare mass of the lepton.[9,10] Thus the effect of virtual photons may be regarded as consisting of two parts: (*A*) the correction to the operator $\bar{\psi}_l a\psi_\nu\varphi_\pi$ due to the dynamical effects of virtual emission of photons, and (*B*) the correction to the coefficient gm_l^0 that arises when one tries to express it in terms of the observed mass m_l.

The correction *A* is found to be

$$\frac{\Delta P_A}{P_0} = \frac{\alpha}{\pi}\left[\tfrac{3}{2}\ln\frac{\lambda}{m_\pi} - b(\mu)\left(\ln\frac{\lambda_{\min}}{m_\pi} - \tfrac{1}{2}\ln\mu + \tfrac{3}{4}\right) + \frac{\mu^2}{1-\mu^2}\ln\mu + \tfrac{1}{2}\right], \tag{7}$$

where λ is the ultraviolet cutoff. Thus, if the correction *B* is disregarded for the moment, the corrected rate of π-e decay is given by

$$P = P_0(1+\eta), \tag{8}$$

where

$$\eta = \frac{\alpha}{\pi}\left[\tfrac{3}{2}\ln\left(\frac{\lambda}{m_\pi}\right) - b(\mu)\ln(1-\mu^2) - \frac{\mu^2(8-5\mu^2)}{2(1-\mu^2)^2}\ln\mu + \frac{2(1+\mu^2)}{1-\mu^2}L(1-\mu^2) + \frac{19-25\mu^2}{8(1-\mu^2)}\right], \tag{9}$$

from (4) to (7). As a matter of fact, it is not necessary to calculate the correction *B* since it is already included in (8) if one remembers that the factor $(m_l^0)^2$ which appears in P_0 is (bare mass)^2 even when the radiative correction is taken into account.

The total decay rate P depends logarithmically on the cutoff λ, but the ratio R of total decay rates for e and μ is independent of the cutoff if it is taken to be the same for both.[11] Under this assumption, the radiative corrections to R_0 of (1) can be expressed as

$$R = R_0(1+\delta)(1+\epsilon), \tag{10}$$

where $1+\delta = [(m_e^0/m_e)/(m_\mu^0/m_\mu)]^2$ comes from correction *B* and $1+\epsilon$ from correction *A* and inner bremsstrahlung. Using the electromagnetic mass of order α, one obtains

$$\delta = -(3\alpha/\pi)\ln(m_\mu/m_e) = -16.0(\alpha/\pi). \tag{11}$$

It is seen from (9) that $\epsilon = -0.92(\alpha/\pi)$ to order α.

Note that there is no physical distinction between correction *A* and correction *B*, their only role being to modify the decay coupling constant. It is therefore misleading to talk of them se-

parately. As is seen from the smallness of ϵ, however, the sum of correction A and inner bremsstrahlung is quite insensitive to whether the decay particle is muon or electron. Thus the radiative correction to R_0 is mostly due to the correction B. In this sense one might say that, when one measures R, one is actually observing a finite difference of electron and muon self-energies.

Ordinarily the experiment looking for π-e decay excludes electrons whose energy is too low, in order to distinguish them from those of π-μ-e decays. Thus we should like to have the ratio $R(\Delta E)$ = (number of π-e decays for which the energy of the electron is within ΔE of the maximum energy)/(number of π-μ decays). This is obtained from (3) and (8). As is easily seen, $R(\Delta E)$ can be written in the same form as (10) where δ is still given by (11) but ϵ now depends on ΔE. The result agrees with Eq. (2) of reference 5.

Numerically, the radiative correction to the ratio R_0 is -3.9% if all decay electrons are counted. Of this value, -3.7% is due to the mass correction (11). Only -0.2% comes from the inner bremsstrahlung and the virtual photon correction A. If only those electrons are observed whose energy is larger than $E_{\max} - \Delta E$, the correction is -7.8% for $\Delta E \sim 10 m_e$ and -14% for $\Delta E \sim 0.5 m_e$. Of these, -3.7% are always due to the mass correction δ. The large negative corrections that still remain are nearly equal in magnitude to the positive probabilities of inner bremsstrahlung (3) which are 3.9% for $\Delta E \sim 10 m_e$ and 10% for $\Delta E \sim 0.5 m_e$. This may be understood qualitatively if one imagines that the probability of finding high-energy electrons is reduced simply because some of them have been shifted to the low-energy side of the spectrum by inner bremsstrahlung. Thus, putting aside the bare mass correction which is energy independent, the large radiative correction found by Berman in $R(\Delta E)$ may be regarded as a consequence of the high efficiency of the π-e system as an emitter of hard photons.

The results of this paper can be qualitatively understood by making use of the "theorem" mentioned at the beginning.[6] At first sight, the radiative correction to π-e decay, although it does not contradict the "theorem," supports it only in a trivial fashion, since not only the total rate but any partial rate of π-e decay vanishes for $m_e \to 0$ because the interaction (5) is proportional to m_e. The fact that the correction δ of (11) diverges logarithmically for $m_e \to 0$ gives no trouble since R_0 tends to zero at the same time. This is in fact expected from our "theorem." It is interesting to note however that the correction ϵ does not diverge in this limit. This can be easily explained by our "theorem," too. For this purpose, we have only to point out that ϵ would be the total radiative correction for pion decay if the interaction were given not by (5) but by

$$f \bar{\psi}_l a \psi_\nu \varphi_\pi, \tag{12}$$

where f is a coupling constant independent of m_l. Since P_0 is now finite for $m_e \to 0$, the correction ϵ cannot afford to diverge if the "theorem" should hold. But (9) is in fact finite for $m_e \to 0$ whereas (3), (4), and (7) diverge. Thus the pion decay gives additional support for the general validity of this conjectured "theorem."

The author would like to thank Professor R. P. Feynman who contributed greatly to this work. He also wishes to thank Dr. S. M. Berman for checking our calculation including the total decay rate.

---

*Supported in part by the joint program of the Office of Naval Research and the U.S. Atomic Energy Commission.

[1]M. A. Ruderman and R. J. Finkelstein, Phys. Rev. 76, 1458 (1949).

[2]M. L. Goldberger and S. B. Treiman, Phys. Rev. 110, 1178 (1958); 111, 354 (1958).

[3]R. P. Feynman and M. Gell-Mann, Phys. Rev. 109, 193 (1958).

[4]T. Fazzini et al., Phys. Rev. Lett. 1, 247 (1958); G. Impeduglia et al., Phys. Rev. Lett. 1, 249 (1958); H. L. Anderson et al., Phys. Rev. Lett. 2, 53 (1959).

[5]S. M. Berman, Phys. Rev. Lett. 1, 468 (1958).

[6]T. Kinoshita and A. Sirlin, 113, 1652 (1959). This "theorem" is conjectured on the basis of our study of radiative corrections to muon decay and beta decay. An attempt is now being made to prove or disprove it for the general case.

[7]The inner bremsstrahlung accompanying pion decay was studied some years ago in connection with observations of anomalously short muon tracks in pion decay. See W. F. Fry, Phys. Rev. 86, 418 (1952). The latest experimental result is reported by C. Castagnoli and M. Muchnik, Phys. Rev. 112, 1779 (1958). For theoretical work, see H. Primakoff, Phys. Rev. 84, 1255 (1951); Nakano, Nishimura, and Yamaguchi, Progr. Theoret. Phys. (Kyoto) 6, 1028 (1951); T. Eguchi, Phys. Rev. 85, 943 (1952).

[8]If the electron mass is neglected in comparison with its energy whenever this approximation does not lead to spurious divergences, the differential spectrum of

electrons is given by

$$dP/P_0 = (\alpha/\pi)(1-x)^{-1}dx\,[(1+x^2)\ln(x/\mu) - 2x - \tfrac{1}{2}(1-x)^2\ln(1-x)],$$

where x is the electron energy measured in units $E_{\max}$. If this is integrated over the range $(0,x)$, one obtains

$$\Delta P_{IB}(x)/P_0 = (\alpha/\pi)\{[2\ln(1-x)+x+\tfrac{1}{2}x^2]\ln(\mu/x) + (\tfrac{3}{4}-\tfrac{1}{2}x+\tfrac{1}{4}x^2)\ln(1-x) + 2L(x) + \tfrac{13}{8}x + \tfrac{1}{8}x^2\}.$$

These formulas are good approximations for any x except at $x \sim 0$. Equation (3), on the other hand, holds only for $\Delta E \ll E_{\max}$, where ΔE is related to x by $x = 1-(2\Delta E/m_\pi)$. Note, however, that no approximation about the electron mass is made in (3), (4), (7), and (9). Thus radiative corrections for π-μ decay are obtained by substituting the observed ratio of pion and muon masses in these formulas.

[9]M. A. Ruderman and W. K. R. Watson, Bull. Am. Phys. Soc. Ser. II, 1, 383 (1956); R. Gatto and M. A. Ruderman, Nuovo cimento 8, 775 (1958).

[10]This is easily proved by rewriting the total Lagrangian making use of the Heisenberg equation of motion for $\bar{\psi}_l$. Obviously (5) and (6) are also equivalent for the inner bremsstrahlung.

[11]If the cutoffs were chosen differently for π-e and π-μ decays, our results concerning virtual photons would become dependent on their ratio ρ. It is interesting to note that measurement of R or $R(\Delta E)$ would determine ρ experimentally if all other assumptions made here were justified.

ABSTRACTS

In this section are printed the abstracts of Articles that have been forwarded to The American Institute of Physics for publication in THE PHYSICAL REVIEW. In quoting information obtained from this section before the appearance of the corresponding Article, reference should be made to "Physical Review (to be published)" rather than to this Journal.

ION CONFINEMENT BY ROTATION IN MAGNETIC MIRROR GEOMETRY. C. L. Longmire, D. E. Nagle, and F. L. Ribe, Los Alamos Scientific Laboratory, University of California, Los Alamos, New Mexico (Received January 8, 1959).

When a generally radial electric field is imposed upon a mirror magnetic field configuration, the resulting system has an increased ability to contain plasma between the mirror regions. The motion of the ions consists of a drift around the axis of symmetry upon which is superimposed a spiralling motion. The guiding center motion departs from the direction of magnetic flux surfaces. An adiabatic invariant is derived for the drift component of the motion, and an expression is derived for the mirror enhancement brought about by the $\vec{E}\times\vec{B}$ drift. The departure of the guiding center of a particle from a flux surface and the energy balance of its secular motion are calculated by using the adiabatic invariant.

EFFECTS OF DISSOLVED GAS ON THE SUPERCONDUCTING CHARACTERISTICS OF TANTALUM. W. B. Ittner, III, and J. Marchand,* Research Laboratory, International Business Machines Corporation, Poughkeepsie, New York (Received January 9, 1959).

The adding of a metallic impurity to a monatomic superconductor is a standard technique employed in experiments where it is desirable to vary systematically some of the material properties of the specimen, e.g., the mean free path or the penetration depth. While it has long been surmized that the addition of a gaseous impurity would produce comparable effects, there has, to our knowledge, been no systematic work carried out to verify this assumption or to measure the magnitude of the effects produced.

We here give a preliminary report on some recent work in which the concentration of a nitrogen contaminant in tantalum has been varied systematically. One effect of the nitrogen contaminant is striking. Very small amounts of gas allow, by a mechanism as yet unknown, for the formation of a "substructure" which permits superconducting inclusions to exist at fields considerably higher than the so-called critical field associated with flux exclusion in the bulk of the specimen. The general behavior of the contaminated specimens is basically the same as that observed in inhomogeneous alloys containing relatively large metallic impurity concentrations. Work is currently in progress to illuminate the basic mechanisms involved in the formation of a substructure in tantalum.

*On leave from the Phillips Company, Eindhoven, Holland.

SECOND LOW-TEMPERATURE PEAK IN THE INTERNAL FRICTION OF ALUMINUM. Edward Lax and Daniel H. Filson, University of California, Los Angeles, California (Received January 12, 1959).

A peak in the internal friction due to dislocations in aluminum was found well below the temperature of the usual Bordoni peak. Measurements were made from 25 kc/sec to above 1 Mc/sec, yielding a relaxation peak that varied with frequency over a temperature range of 21°K to 31°K. The activation energy of this peak was found to be 0.024 ev.

ELECTRON SPIN RESONANCE EXPERIMENTS ON DONORS IN SILICON. I. ELECTRONIC STRUCTURE OF DONORS BY THE ELECTRON NUCLEAR DOUBLE RESONANCE TECHNIQUE. G. Feher, Bell Telephone Laboratories, Murray Hill, New Jersey (Received December 29, 1958).

The ground state wave function of the antimony, phosphorus, and arsenic impurities in silicon has been investigated by means of the electron nuclear double resonance (ENDOR) method. By this method the hyperfine interactions of the donor electron with the Si^{29} nuclei situated at different lattice sites were obtained. The isotropic part of the hyperfine interaction agreed with the theory of Kohn and Luttinger to better than 50%. From a comparison of the experimental results with their theory a value for the conduction band minimum in silicon of $k_0/k_{max} = 0.85 \pm 0.03$ was obtained. So far no satisfactory theory exists to account quantitatively for the

observed anisotropic part of the hyperfine interaction.

The observed line shape agreed with the shape predicted by summing up the individual hyperfine interactions which are the cause of the broadening. The behavior of an inhomogeneously broadened line observed under adiabatic fast passage conditions is discussed in an appendix. The electronic g-values were measured with respect to the free carriers in a degenerate n-type silicon sample. The g-value of the free carriers was found to be 1.99875 ± 0.00010. The deviations of the donor g-values from the above value is several parts in 10^4 and increases monotonically with increasing ionization energy of the donors.

Besides the shallow donors Sb, P, and As, several other centers were investigated, but in considerably less detail. They include the chemical impurities Bi, Li, Fe, centers associated with the surface of the sample and with the heat treatment of silicon. The influence of substitutional germanium atoms on the resonance line in phosphorus-doped silicon has also been investigated.

ELECTRON SPIN RESONANCE EXPERIMENTS ON DONORS IN SILICON. II. ELECTRON SPIN RELAXATION EFFECTS. G. Feher and E. A. Gere, Bell Telephone Laboratories, Murray Hill, New Jersey (Received December 29, 1958).

The different relaxation processes that connect the four energy levels in phosphorus-doped silicon have been investigated experimentally. The relaxation time T_S ($\Delta m_S = \pm 1$, $\Delta m_I = 0$) was found to be independent of phosphorus concentration below $\sim 10^{16}$ P/cm^3. Its value at 3200 oersteds and 1.25°K was $\sim 3 \times 10^{+3}$ seconds and varied as $1/T$ for $1.3°K < T < 2°K$ and as $1/T^7$ for $2.5°K < T < 4.2°K$. The magnetic field dependence in the $1/T$ region suggests a direct phonon process. In the $1/T^7$ region T_S was independent of the magnetic field between 3000 and 8000 oersteds. Above a concentration of 10^{16} P/cm^3, T_S varied rapidly with donor concentration, dropping to 10^{-4} second at 3×10^{17} P/cm^3. In this concentration-dependent region, T_S was independent of the magnetic field but depended on the number of acceptors present. None of the T_S mechanisms can at present be accounted for by the theories of Pines, Bardeen, and Slichter, and Abrahams. The relaxation time T_X ($\Delta m_S = \pm 1$, $\Delta m_I = \mp 1$) was ~30 hours at 3000 oersteds and ~5 hours at 8000 oersteds in fair agreement with the theory of PBS. The relaxation time T_N ($\Delta m_I = \pm 1$, $\Delta m_S = 0$) at 1.25°K exceeded 10 hours.

The effect of light was investigated with a monochromator for $0.5 \text{ ev} < h\nu < 2 \text{ ev}$. The number of carriers introduced by light was obtained from the Hall coefficient. In a sample with 7×10^{15} P/cm^3, T_S was reduced to 25 seconds by 2×10^6 electrons/cm^3. Under the same conditions the spin-spin time T_{SS} was reduced to 1 second. The bottleneck in the T_S-spin exchange mechanism suggested by Pines, Bardeen, and Slichter is the spin-lattice relaxation time of the free carriers. This bottleneck is absent in a double spin exchange mechanism suggested by Anderson and is responsible for the observed T_{SS} process.

A resonant spin-spin interaction was observed between the electron bound to an iron impurity and the phosphorus donor electron when the magnetic field at which the two resonance lines overlap was traversed. The application of this "mixing" effect to a nuclear polarization scheme is discussed. A complete mixing of two levels was also observed in phosphorus-doped silicon at a magnetic field of 40 oersteds.

A spin diffusion process capable of transmitting a spin excitation to different parts of the resonance line was observed in arsenic-doped silicon. This process proceeds in discrete steps with frequencies determined by the different Larmor frequencies of the Si^{29} nuclei situated at various lattice sites relative to the donor atom.

POLARIZATION OF THE ELECTRON GAS IN METALS BY SUBSTITUTIONAL IMPURITIES. B. D. Silverman* and P. R. Weiss, Physics Department, Rutgers University, New Brunswick, New Jersey (Received December 17, 1958).

The ground-state energy of the system of impurities and conduction electrons in a metal has been obtained in the limit of high electron density. The procedure used is an extension of the Wentzel method applied to a reduced Hamiltonian which includes an electron-impurity interaction. It is reduced in the sense that the Coulomb interaction between electrons and the electron-impurity interaction are only effective in raising an electron in a state below the Fermi level to one above and vice versa. The ground-state energy is then obtained by a canonical transformation. The shift in energy of the ground state of the electron gas, due to the introduction of the

impurities, is quadratic in the electron-impurity matrix element. Higher order processes in this matrix element do not contribute since they are represented by unlinked diagrams. Considering this shift in the ground-state energy to be expandable in powers of r_s, a measure of the average interelectronic distance, we show the leading or lowest order term in this parameter to go as $(n/n_e)r_s^{-1/2}$, where n is the impurity density and n_e the electron density. Impurity locations are assumed random. All processes omitted in the reduction of the Hamiltonian are shown to contribute to higher powers in r_s. The role of exchange is indicated.

*Now at the Research Division, Raytheon Manufacturing Company, Waltham, Massachusetts.

SYMMETRY OF WURTZITE. R. C. Casella, Research Laboratory, International Business Machines Corporation, Poughkeepsie, New York (Received December 29, 1958).

The symmetry analysis of wurtzite, performed originally by Dresselhaus at the origin of the Brillouin zone, is extended. A method is employed at the zone boundaries which is considerably simpler than the standard procedure. Optical selection rules for band-to-band transitions in the neighborhood of $k=0$ are re-examined. It is found that light polarized perpendicular to the c axis should be absorbed more strongly than light polarized along the c axis, independently of the symmetry types of the initial and final states, unless they have the same symmetry, which is unlikely. This result is in agreement with experiment for CdS and ZnS.

SOME SELECTION RULES FOR BAND-BAND TRANSITIONS IN WURTZITE STRUCTURE. Joseph L. Birman, Sylvania Research Laboratories, Bayside, New York (Received January 23, 1959).

Optical selection rules at $\vec{k}=(0,0,0)$ in the wurtzite structure are discussed. These rules suggest an interpretation of recently reported work on CdS by Dutton and Lempicki on reflection spectra, and the excitation spectrum of edge emission in polarized light. Assuming band-band transitions at $\vec{k}=(0,0,0)$ are involved, a valence band spin-orbit splitting of 0.0167 ev and crystal field splitting of about 0.070 ev (at liquid N_2 temperature) are obtained for CdS. Other predictions of the model and other possible interpretations of the data are discussed.

CHANGE IN VELOCITY OF SOUND BETWEEN NORMAL AND SUPERCONDUCTING STATES IN TIN. D. F. Gibbons and C. A. Renton, Bell Telephone Laboratories, Murray Hill, New Jersey (Received January 8, 1959).

The difference in the velocity of sound between the normal and superconducting state in tin was measured at 80 kc/sec. A maximum change of ~ 2 parts in 10^6 is found for a longitudinal wave in the [001] direction. Any change in velocity is < 2 parts in 10^7 for a longitudinal wave along the [100] direction or a torsional wave along the [001] direction. This disagrees with some previous determinations, but is in accord with other thermodynamic measurements. The effect of strain amplitude and magnetic field on the velocity and attenuation of the sound wave in the normal state has also been investigated in some detail.

IMPURITY EFFECTS ON THE SUPERCONDUCTIVE CRITICAL TEMPERATURE OF INDIUM AND ALUMINUM. G. Chanin, E. A. Lynton, and B. Serin, Department of Physics, Rutgers University, New Brunswick, New Jersey (Received December 10, 1958).

We find that the effects of 0.01 to 1.0 atomic percent of various impurities on the superconductive critical temperature of indium and aluminum are strikingly similar to those previously reported for tin. For sufficiently small amounts of all solutes there is an electronic mean free path effect on the critical temperature such that T_c decreases linearly with increasing reciprocal free path. For larger impurity concentrations the curves of critical temperature versus concentration fall into groups according to the valence difference between solvent and solute. T_c has a sharp upward trend for higher valence solutes; for those with lower valence the curves of T_c tend to flatten out. The similarity of these impurity effects for three such different superconductors suggests that they are a fundamental property independent of the detailed nature of the superconductor.

ELECTRON CHARACTERISTIC ENERGY LOSSES IN SOME INTERMETALLIC COMPOUNDS. Bernard Gauthé,* National Bureau of Standards, Washington, D. C. (Received January 7, 1959).

Measurements have been made of the characteristic energy losses of 30-kev electrons in transmission through thin films of indium, indium antimonide, cadmium telluride, and zinc telluride; for comparison, the electron energy losses in antimony, cadmium, tellurium, and zinc have been reinvestigated. The energy loss spectra in these intermetallic compounds appear significantly different from a simple superposition or average of the energy loss spectra of the component metals. Some detailed interpretations of the characteristic energy losses in In and in InSb are suggested.

*On leave of absence from the Laboratoire de Chimie-Physique, University of Paris, Paris, France.

K X-RAY SPECTRUM OF Hg. Olof Beckman and Pär Bergvall, Institute of Physics, Uppsala, Sweden (Received December 22, 1958).

The *K* x-ray spectrum of Hg has previously not been measured with the same accuracy as nearby elements because of the difficulty of obtaining a good anticathode. A wavelength determination of Hg *K* α_1, α_2, β_1, and β_3 is herewith reported with an accuracy of less than 40 parts per million. Using these data an earlier measurement of the weaker Hg lines is recalculated to give higher accuracy.

LOW-FIELD MOBILITIES OF THE NEGATIVE IONS IN OXYGEN, SULFUR HEXAFLUORIDE, SULFUR DIOXIDE, AND HYDROGEN CHLORIDE. E. W. McDaniel, Engineering Experiment Station and School of Physics, Georgia Institute of Technology, Atlanta, Georgia, and M. R. C. McDowell, Royal Holloway College, University of London, Englefield Green, Surrey, England (Received October 7, 1958).

Measurements of the low-field mobility of the negative ions in O_2, SF_6, SO_2, and HCl are described. The results are 2.46, 0.57, 0.35, and 0.71 cm^2/v sec, respectively, reduced to 0°C and 760 mm Hg pressure. A quantum mechanical theory of ionic mobility is outlined and applied to the gases investigated experimentally. Comparison of the experimental and theoretical results indicates that the oxygen ion is O_3^-, but attempts to identify the ions in the other gases are inconclusive.

MICROWAVE ZEEMAN SPECTRUM OF ATOMIC OXYGEN. H. E. Radford and V. W. Hughes, Sloane Physics Laboratory, Yale University, New Haven, Connecticut (Received December 1, 1958).

The technique of paramagnetic resonance absorption has been used to measure the g-factors of the ground ^3P term in O^{16} in terms of the proton g-factor. The results are: $-g_J(O;\ ^3P_1)/g_p = 493.4236 \pm 0.0002$ and $-g_J(O;\ ^3P_2)/g_p = 493.4022 \pm 0.0002$, where g_p refers to protons in a cylindrical sample of mineral oil. When combined with $g_J(H;\ ^2S_{1/2})/g_p$ measured in analogous experiments on hydrogen, and after inserting the theoretical value of $g_J(H;\ ^2S_{1/2})$, the oxygen g-factors are found to be $g_J(O;\ ^3P_1) = 1.500986 \pm 0.000002$ and $g_J(O;\ ^3P_2) = 1.500921 \pm 0.000002$. A discrepancy of 7 parts in 10^6 between these values and corresponding theoretical g-factors can probably be laid to inaccuracy of the atomic wave functions used in the theoretical calculations.

DETERMINATION OF ELECTRON POLARIZATION BY MEANS OF MOTT SCATTERING. Noah Sherman and Donald F. Nelson, Physics Department, University of Michigan, Ann Arbor, Michigan (Received January 8, 1959).

The results of a numerical calculation of the polarization asymmetry factor, $S(\theta) = [\delta(\theta)]^{1/2}$, and the single scattering cross section for the scattering of electrons by the unscreened Coulomb fields of gold and aluminum at energies of 75 kev and 121 kev are presented. The results for gold at 121 kev are compared with the Mohr and Tassie calculations for the same element and energy which include the effects of screening. This comparison (indicating a Mott asymmetry about 50% greater for the screened field at angles near 165°) suggests the desirability of more detailed investigation of screening effects in order to be confident of Mott scattering as a means of measuring the polarization of electrons in this energy region.

RATIO OF THE GAMOW-TELLER AND FERMI COUPLING CONSTANTS DETERMINED FROM *ft* VALUES. O. C. Kistner and B. M. Rustad, Columbia University, New York, New York, and Brookhaven National Laboratory, Upton, New York (Received January 9, 1959).

A comparison is made of the ratios of the squares of the Gamow-Teller and Fermi coupling constants, C_{GT}^2/C_F^2, calculated from the latest experimental *ft* values and the theoretical matrix elements for the "doubly closed shell ± 1 nucleon" mirror transitions and the 0^+-0^+ transitions. The *ft* value of the neutron derived from the recent half-life measurement of 11.7±0.3 minutes leads to a value for C_{GT}^2/C_F^2 of 1.42±0.06, which is in agreement with the ratio obtained from the correlation coefficient for the beta-particle momentum and the spin direction of the decaying neutron. The *ft* value for the decay of H^3 is also in good agreement with this ratio if the Gamow-Teller matrix element for this transition does not differ appreciably from that predicted by the individual particle model. The *ft* values of the heavier mirror nuclei, O^{15}, F^{17}, and Ca^{39}, are consistent with a considerably lower ratio. In particular, O^{15} and F^{17}, for which the Gamow-Teller matrix elements are considered the most reliable because the magnetic moments of the daughter nuclei are especially close to the Schmidt limits, lead to a value for C_{GT}^2/C_F^2 of 1.16±0.05. These results are consistent with recent theoretical considerations which suggest that meson exchange effects may give rise to appreciable corrections in the calculation of the matrix elements.

NOTE ON THE PHOTODISINTEGRATION OF THE DEUTERON. W. Zernik, M. L. Rustgi, and G. Breit, Yale University, New Haven, Connecticut (Received January 12, 1959).

The differential cross section $\sigma(\theta,\varphi)$ and proton polarization $P(\theta,\varphi)$ have been computed at γ-ray energies of 22.5, 32.8, 64.4, 107.8, 164.5, and 193.9 Mev. The nuclear force potential was a slightly modified form of that used by Signell and Marshak. In order to test recent claims regarding comparison with experiment not calling for the inclusion of effects of retardation and exchange currents, these effects have been neglected. The influence of the inclusion of different multipoles has been studied by employing successive approximations in which the transitions which are unimportant at low energies are introduced in turn. The inclusion of $M1$ transitions to triplets and of $E2$ effects has left discrepancies of several times the experimental error with data on σ at 65 and 108 Mev. The relative largeness of the effects of the transitions just mentioned at the higher energies complicates the employment of the photoeffect as a means of obtaining evidence regarding the nucleon-nucleon interaction.

LIFETIME OF THE 3.56-Mev STATE IN Li^6. R. J. A. Levesque* and S. M. Shafroth, Northwestern University, Evanston, Illinois (Received January 12, 1959).

An upper limit for the mean life of the 3.56-Mev state in Li^6 of 5×10^{-14} sec has been established by a Doppler-shift method. This supports the 0^+, $T=1$ assignment for this level. It has also been established by a Doppler-shift technique that the angular distribution of the recoil alpha particles arising from the $Be^9(p,\alpha)Li^{6*}(\gamma)Li^6$ reaction is symmetric about 90° in the center-of-mass system at the resonant bombarding energy of 2.56 Mev. At 2.93-Mev bombarding energy the angular distribution of the alpha particles is peaked forward of 90°.

*Present address: Physics Department, University of Maryland, College Park, Maryland.

0- to 0+ BETA TRANSITION: Pr^{144}–Nd^{144}. Fred T. Porter and Paul P. Day, Argonne National Laboratory, Lemont, Illinois (Received January 14, 1959).

The Argonne double-lens beta spectrometer and associated coincidence circuit have been used to observe the beta transitions of Pr^{144}. The validity of the spin and parity assignment, 0-, to Pr^{144} is supported by a measurement of the shape of the (1.2±0.1)% abundant 2.3-Mev beta transition, observed in coincidence with the 697-kev gamma ray. Its shape is that of the unique ($\Delta I=2$, yes) first forbidden transition expected if the transition goes from 0- Pr^{144} to the 2+ first excited state of even-even Nd^{144}. The shape of the (1.0±0.1)% abundant (807±5)-kev beta transition to the 2.19-Mev level in Nd^{144} was observed in coincidence with the 1.49- and

2.19-Mev gamma rays. Its allowed shape is consistent with a 0- assignment for Pr^{144}. With this assignment the transition between the ground states is a 0- to 0+ case. The shape of this (2996 ± 3)-kev, 97.8% abundant, transition was obtained from the total spectrum by small subtractions of the inner groups. Its nearly allowed shape is easily explained with a pure axial vector shape factor; in contrast, the tensor-pseudoscalar formalism fails to reproduce the shape. The ratio of axial vector matrix elements $\lambda = (i\int\gamma_5/\int\vec{\sigma}\cdot\vec{r})$ can be determined from the shape; our data give $\lambda = 5 \pm 2$. This is the same absolute magnitude as some theoretical estimates but has the opposite sign. Our experimental results are in good agreement with those of Graham, Geiger, and Eastwood who have already pointed out that this 0- to 0+ transition does not offer a sensitive measure of the relative size of pseudoscalar to axial vector coupling constants although the net relative contribution of the direct pseudoscalar part to the whole AP shape factor must be $\leq 1\%$ (with Rose-Osborne formalism).

An incidental result of the present work is that the $H\rho$ of the K conversion line of the 133.5-kev transition following the β decay of Ce^{144} has been measured as 1064.8 ± 0.6 gauss cm.

GAMMA RAYS FROM THE 1.83-Mev RESONANCE IN THE REACTION $Mg^{24}(p,\gamma)Al^{25}$. A. E. Litherland, H. E. Gove and A. J. Ferguson, Atomic Energy of Canada Limited, Chalk River, Ontario, Canada (Received January 12, 1959).

The $Mg^{24}(p,\gamma)Al^{25}$ reaction has been studied in the range of proton energies from 1.66 Mev to 2.02 Mev. A new resonance at 1.833 ± 0.007 Mev was observed which corresponds to an excited state of 4.047 ± 0.010 Mev in Al^{25}. The new excited state was observed to decay by the emission of 4.01 ± 0.04, 2.43 ± 0.04, and 1.62 ± 0.03 Mev gamma rays. The last two gamma rays were observed to be in coincidence and the intensity ratio of the first two gamma rays was found to be (60 ± 10):(40 ± 10). The experimental value of $\omega\gamma = (J+\frac{1}{2})\Gamma_p\Gamma_\gamma/\Gamma$ was found to be 3×10^{-3} ev for the ground-state transition and an upper limit of 10 kev was estimated for Γ, the total width of the resonance. Angular distribution measurements have shown that the angular momentum of the new state is either 5/2 or 9/2, with the latter value favored. On the basis of the observed dipole-quadrupole admixtures found for the gamma rays, the parity of the new state is probably even. A discussion is given of the place of the new state in the rotational-like bands of Al^{25}.

DECAY OF $I^{130} - Xe^{130}$. W. G. Smith,* P. H. Stelson, and F. K. McGowan, Oak Ridge National Laboratory, Oak Ridge, Tennessee (Received January 9, 1959).

The decay of I^{130} has been previously studied by two groups of workers, and, as a result, the following level scheme for Xe^{130} has been proposed: 528 kev (2^+), 1190 kev (4^+), 1930 kev (6^+), and 2340 kev (5^-). Only the states at 1930 kev and 2340 kev were found to be directly populated by beta decay. However, the recent measurement of spin 5 for I^{130} suggests that the 1190-kev state, if 4^+, should be populated by beta decay. In the present work, such a group was looked for and not found. A lower limit of 9.8 was set for the logft. Gamma-gamma correlations were also made. The experimental correlation for 1190-528-0 level sequence can be fitted by $4(Q)2(Q)0$ or by 2(96% D + 4% Q)$2(Q)0$ sequences. The 2^+ assignment to the 1190-kev level requires a predominantly $M1$ transition for the 2^+ to 2^+ transition in contrast to the predominantly $E2$ character of other known transitions of this type. Therefore, either 4^+ or 2^+ assignment to the 1190-kev state leads to an anomalous situation. Six other angular correlations were measured in an attempt to determine the characteristics of the levels at 1930 kev and 2340 kev. It was not possible to obtain unique assignments.

*Summer research participant from Purdue University, Lafayette, Indiana.

$B^{11}(He^3,p)C^{13}$ AND $B^{11}(He^3,d)C^{12}$ REACTIONS. H. D. Holmgren, E. A. Wolicki, and R. L. Johnston, Nucleonics Division, United States Naval Research Laboratory, Washington, D. C. (Received January 5, 1959).

The differential cross sections for the $B^{11}(He^3, p)C^{13}$ and the $B^{11}(He^3,d)C^{12}$ reactions have been measured at 4.5 and 5.4 Mev. Yield curves for these reactions have also been obtained over the energy region extending from 3.00 to 5.40 Mev. The angular distributions for the deuteron groups are strongly peaked in the forward direction and indicate that the simple stripping interaction is

the predominant mechanism of these reactions. The angular distributions of the proton groups are more complex and more difficult to interpret; however, the yield curves change rather slowly with energy, suggesting that direct interaction mechanisms may be important.

ANALYSIS OF PHOTONUCLEAR CROSS SECTIONS. A. S. Penfold, Enrico Fermi Institute for Nuclear Studies, University of Chicago, Chicago, Illinois, and J. E. Leiss, National Bureau of Standards, Washington, D. C. (Received December 15, 1958).

The problem of obtaining a photonuclear cross section from a yield curve measured with a bremsstrahlung beam is discussed. This paper constitutes part of a larger report on the same subject containing numbers enabling cross-section analysis in the energy range 2 Mev to 1 Bev.

NUCLEAR PHOTON ABSORPTION IN CARBON AND OXYGEN. A. S. Penfold and E. L. Garwin, Enrico Fermi Institute for Nuclear Studies, University of Chicago, Chicago, Illinois (Received January 15, 1959).

The importance of narrow, isolated, resonances in the photonuclear absorption cross sections of C and O was investigated by means of an absorption experiment performed with 30.7 Mev bremsstrahlung. The experiment yielded values for the cross sections averaged over the (γ,n) cross sections for C^{12} and O^{16}. The results for C were the same as those expected for a cross section without narrow resonances, while for O a definite resonance effect was demonstrated. The O photonuclear absorption cross section, averaged over the $O^{16}(\gamma,n)O^{15}$ cross section, was found to be 26.7 ± 3.5 millibarns, 16 ± 4 millibarns higher than the value expected if narrow resonances contribute insignificantly. Estimated values for the parameters of the O resonances near 22 Mev are: average peak height, 106 ± 14 millibarns; ratio of the radiative width (to ground state) to total width, $(6.6 \pm 0.9) \times 10^{-3}$; total width about 30 kev. The experimental results are insensitive to uncertainties in the non-nuclear x-ray attenuation cross sections for C and O.

PRECISION MEASUREMENT OF THE $Be^9(\gamma,n)$ CROSS SECTION. J. H. Gibbons, R. L. Macklin, J. B. Marion,* and H. W. Schmitt, Oak Ridge National Laboratory, Oak Ridge, Tennessee (Received January 5, 1959).

Measurements have been made of the photoneutron production cross section for Be^9 using γ rays from radioactive sources of Y^{88} (1.85 Mev) and Sb^{124} (1.69 Mev). The values obtained at these two energies are $(6.54 \pm 0.31) \times 10^{-28} cm^2$ and $(12.62 \pm 0.69) \times 10^{-28} cm^2$, respectively. The limiting factors in the accuracy of these measurements are the uncertainties in the γ-ray source strength calibration and in the NBS No. 2 Ra-γ-Be neutron source standard, and the lack of precise knowledge concerning the Sb^{124} decay scheme. A new measurement of the γ-ray branching ratios in the Sb^{124} decay has also been made.

*Permanent address: University of Maryland, College Park, Maryland.

PROTON ELASTIC SCATTERING CROSS SECTIONS OF Si, Cl, K, Sc, Ti, AND Mn. Sylvan Rubin, L. Evan Bailey, and Thomas O. Passell, Stanford Research Institute, Menlo Park, California (Received December 23, 1958).

The proton elastic scattering yields of silicon, chlorine, potassium, scandium, titanium, and manganese have been determined with respect to that from copper in the energy range 1.0-2.0 Mev at 150° laboratory angle. Two large resonances were found in silicon and two smaller ones in chlorine. The smooth regions of the curves do not vary significantly from the Rutherford values.

γ-RAYS FOLLOWING THERMAL NEUTRON CAPTURE IN TITANIUM. J. W. Knowles, G. Manning,* G. A. Bartholomew, and P. J. Campion, General Physics Branch, Atomic Energy of Canada Limited, Chalk River, Ontario, Canada (Received December 18, 1958).

The γ-rays following thermal neutron capture in titanium have been studied with two high-resolution spectrometers and with an angular correlation arrangement using two sodium iodide scintillation spectrometers. The high-resolution instruments were a pair spectrometer for the energy range

2.8 to 11.0 Mev and a double flat crystal diffraction spectrometer for the energy range 0.14 to 5 Mev. A total of 54 gamma rays were observed, 25 of which had not previously been resolved. A decay scheme for Ti^{49} is given with energy levels at 1.378 ± 0.001, 1.583 ± 0.001, 1.719 ± 0.001, 3.172 ± 0.002, and 3.261 ± 0.005 Mev. The neutron binding energy of Ti^{49} is concluded to be 8.132 ± 0.006 Mev. Angular correlation measurements were made between some of the prominent γ rays emitted in the decay of Ti^{49}. The measurements confirm that the spins of the 1.378- and 1.719-Mev levels are 3/2 and 1/2, respectively.

*Now at Norman Bridge Laboratory of Physics, California Institute of Technology, Pasadena, California.

PHOTOPROTON CROSS SECTIONS OF CARBON. S. Penner and J. E. Leiss, National Bureau of Standards, Washington, D. C. (Received December 31, 1958).

The partial (γ,p) cross section of carbon in which the residual boron nucleus is left in the ground state has been measured with a thin-crystal proton spectrometer. This cross section is shown to decrease from about 10 mb at the giant resonance peak (22 Mev) to about 0.1 mb near 60 Mev photon energy. Angular distributions measured at five energies exhibit an asymmetry around 90° which increases rapidly with increasing energy. The partial cross section to the first excited state of boron is (7 ± 16) % of the ground-state cross section. The partial cross section to one or more excited states of boron about 5 Mev above the ground state is comparable with the ground-state cross section above 30 Mev photon energy. In addition to the cross-section data, the measurements provide a sensitive means of calibrating the energy scales of electron accelerators at energies in the 25 to 50 Mev region.

SCATTERING OF 14-Mev NEUTRONS BY CARBON. John B. Singletary* and Donald E. Wood,† Northwestern University, Evanston, Illinois (Received January 9, 1959).

Differential and total cross sections have been determined for scattering of 14.1-Mev neutrons from several levels in carbon. The data were measurements of scattered neutrons made by means of the proton recoil reaction in nuclear emulsion plates. The inelastic cross sections were 203 mb for the 4.4-Mev level, 96 mb for the 9.6-Mev level, and 124 mb for the unresolved higher levels. The shape of the angular distribution for the 4.4-Mev level indicated the possibility of some direct interactions. No significant amount of scattering was observed due to the 7.6-Mev level. The elastic scattering angular distribution showed a forward-peaked diffraction-type structure and yielded a cross section of 805 mb. Comparisons are made with other data on the elastic and 4.4-Mev level scattering.

*Now at the Los Alamos Scientific Laboratory, Los Alamos, New Mexico.
†Now at General Electric Company, Hanford Laboratories, Richland, Washington.

SLOW NEUTRON RESONANCES IN Eu^{151} AND Eu^{153}. Fahri Domanic* and Eugene T. Patronis, Jr., Brookhaven National Laboratory, Upton, New York (Received December 9, 1958).

The total neutron cross sections of Eu^{151} and Eu^{153} have been measured between 1 and 10 ev using a high-resolution crystal spectrometer. The Breit-Wigner parameters have been obtained for the 1.055-, 2.717-, 3.368-, and 3.710-ev resonances in Eu^{151}, and for the 1.725-, 2.456-, 3.294-, 3.944-, 6.16-, and 8.87-ev resonances in Eu^{153}. The values of the radiation widths for the 1.055-, 2.717-, 3.368-, and 3.710-ev resonance in Eu^{151} are almost identical, whereas out of the six resonances in Eu^{153} five are almost identical, and one is about 30% higher.

*On leave from the University of Ankara, Ankara, Turkey.

PRECISE DETERMINATION OF THE U^{233} FISSION NEUTRON SPECTRUM. A. B. Smith, P. R. Fields, and R. K. Sjoblom, Argonne National Laboratory, Lemont, Illinois, and J. H. Roberts, Northwestern University, Evanston, Illinois (Received December 22, 1958).

The U^{233} prompt fission neutron spectrum is measured. Fast time of flight techniques are employed to study the neutron energy distribution from 0.3 to 5.0 Mev. Proton recoil emulsions are utilized for neutron measurements

from 1.2 to 7.0 Mev. The experimentally determined fission neutron spectrum is expressed in the form: $N(E) = (a_0 + a_1E + a_2E^2)\phi(E)$, where E is the neutron energy in Mev, $N(E)$ is the number of U^{233} fission neutrons per unit energy interval, $\phi(E)$ is the U^{235} prompt fission neutron spectrum, and a_0, a_1, and a_2 are constants normalized to give agreement with the known average number of U^{233} prompt fission neutrons. The average energy of the U^{233} prompt fission neutrons calculated from the experimental results is 1.87 ±0.04 Mev.

DEVIATION FROM THE ξ APPROXIMATION IN THE FIRST FORBIDDEN β DECAY. Tsuneyuki Kotani,* Department of Physics, Indiana University, Bloomington, Indiana (Received November 19, 1958).

The failure of the ξ approximation is due to either the cancellation or selection rule effect. The latter may be due to K or j forbiddenness. In order to distinguish these three possibilities experimentally, the two transitions, $3(\beta)2(\gamma)0$ and $2(\beta)2(\gamma)0$, are discussed. The present data on Sb^{124} and Rb^{86} are insufficient to permit drawing a definite conclusion. Similar arguments can be extended to other β decays. To get more information, the general energy and angular dependences are given in convenient form for various observables, and are shown numerically for Sb^{124}. Certain β-γ correlation experiments, especially the β–circularly polarized γ correlation and the transverse β polarization, are proposed for a variety of special β decays, e.g., Ga^{72}, Y^{92}, and so on. It is also concluded that the unique-shape energy spectrum does not necessarily correspond to a unique forbidden transition. An example is Eu^{152}. Measurements of β-γ correlations are useful in order to decide this correspondence. Other β decays, which may be characterized by the cancellation, are Ag^{111}, Re^{186}, and Tm^{170}.

*On leave from Tokyo Metropolitan University, Setagaya, Tokyo.

TRIDENTS, μ-PAIRS, AND QUANTUM ELECTRODYNAMICS AT SMALL DISTANCES. J. D. Bjorken and S. D. Drell, Department of Physics and Institute of Theoretical Physics, Stanford University, Stanford, California (Received January 12, 1959).

Four experiments are proposed and discussed as tests of quantum electrodynamics, as applied to photons, electrons, and μ mesons at distances $< 10^{-13}$ cm. These are: (1) electron-positron pair production by electrons in hydrogen (tridents); (2) wide-angle photoproduction of μ-meson pairs in hydrogen with detection of one final meson; (3) wide-angle photoproduction of μ-meson pairs in hydrogen with detection of both final mesons in coincidence; (4) μ-meson pair-production by electrons in hydrogen. Taken together with wide-angle photoproduction of electron-positron pairs, which was discussed earlier, these experiments will extend our knowledge of electron, photon, and μ-meson "size" to distances $\sim 0.3 \times 10^{-13}$ cm. They are all feasible for the Stanford linear accelerator operating in the 500-Mev–1-Bev energy range.

NUCLEAR ABSORPTION CROSS SECTIONS FOR 3.6-Bev NEUTRONS. Paul H. Barrett, University of California, Santa Barbara, California (Received January 5, 1959).

The absorption cross sections for neutrons on Pb, Cu, and Al have been measured by means of poor-geometry transmission measurements. The neutrons were produced by bombarding a 1-in. thick polyethylene target with 6.2-Bev protons in the Bevatron. Neutron detection was accomplished by measuring the density of stars in nuclear emulsion. These measurements gave for the absorption cross sections for Pb, Cu, and Al 1930 ± 300 mb, 704 ± 140 mb, and 430 ± 56 mb, respectively. An absorption mean free path in emulsion of $\lambda = 50 \pm 10$ cm was obtained. The source strength of the neutrons was calculated to be 0.19 (neutron/steradian) per proton striking the target. By comparing the multiplicity of mesons produced in nuclear interactions by the neutron beam and by protons of known energy, the average energy of 3.6 ± 0.7 Bev was obtained for the neutron beam.

ELASTIC PROTON-DEUTERON SCATTERING AT 450 Mev. A. V. Crewe,* B. Ledley, E. Lillethun, S. Marcowitz, and L. G. Pondrom,† Enrico Fermi Institute for Nuclear Studies, Uni-

versity of Chicago, Chicago, Illinois (Received January 9, 1959).

The elastic scattering cross section for 450-Mev protons by deuterons has been measured for proton center-of-mass scattering angles from 16.45° to 127°. The scattered protons (or recoil deuterons) were analyzed by a magnet and detected by a scintillation counter telescope. The cross sections have been normalized by using published p-p cross sections. The sticking factor has been calculated for two deuteron potentials using the impulse approximation. This analysis indicates that there may be destructive interference between the n-p and p-p scattering in the deuteron at this energy.

*Also at Argonne National Laboratory, Lemont, Illinois.

†Now at Wright-Patterson Air Force Base, Dayton, Ohio.

GEOMETRICAL SIGNIFICANCE OF THE EINSTEIN-MAXWELL EQUATIONS. Gerald Rosen, Palmer Physical Laboratory, Princeton, New Jersey (Received December 22, 1958).

Rainich geometries are analyzed in terms of the invariants associated with the Ricci vierbein of principal directions. At any point the four unit vectors of the vierbein pair off into two blades which contain the maxima and minima directions of mean curvature, respectively. The blades can "mesh" into smooth integral surfaces for certain electromagnetic fields. In general, neighboring blades are shown to be related by only two independent differential conditions.

PARITY OF THE K MESON AND THE Λ BETA-DECAY BRANCHING RATIO. C. H. Albright, Palmer Physical Laboratory, Princeton University, Princeton, New Jersey (Received January 7, 1959).

The related problems of Λ beta decay and $K_{\mu 2}$ decay (via a Λ-antiproton loop) are studied. Dispersion techniques are used to calculate the vector (axial vector) Fermi interaction coupling constant from the known $K_{\mu 2}$ lifetime and reasonable values of the strong-coupling constant for the scalar (pseudoscalar) K case. Each weak-coupling constant is then used to place a lower limit on the Λ beta-decay branching ratio with the result that the limit with a pseudoscalar K is more than one order of magnitude smaller than that with a scalar K meson. The present meager experimental information is essentially consistent with either K parity, for the observed branching ratio is approximately equal to the lower limit predicted for the scalar K case.